Systemic paralogy and function of retinal determination network homologs in arachnids

*Guilherme Gainett[1], *Jesús A. Ballesteros[1], Charlotte R. Kanzler[1], Jakob T. Zehms[1], John M. Zern[1], Shlomi Aharon[2], Efrat Gavish-Regev[2], Prashant P. Sharma[1]

[1]Department of Integrative Biology, University of Wisconsin-Madison, Madison, WI, USA 53706

[2] National Natural History Collections, The Hebrew University of Jerusalem, Jerusalem, Israel

*Equal author contribution

Correspondence: guilherme.gainett@wisc.edu, ballesterosc@wisc.edu

Abstract

Arachnids are important components of cave ecosystems and display many examples of troglomorphisms, such as blindness, depigmentation, and elongate appendages. Little is known about how the eyes of arachnids are specified genetically, let alone the mechanisms for eye reduction and loss in troglomorphic arachnids. Additionally, paralogy of Retinal Determination Gene Network (RDGN) homologs in spiders has convoluted functional inferences extrapolated from single-copy homologs in pancrustacean models. Here, we investigated a sister species pair of Israeli cave whip spiders (Arachnopulmonata, Amblypygi, *Charinus*) of which one species has reduced eyes. We generated the first embryonic transcriptomes for Amblypygi, and discovered that several RDGN homologs exhibit duplications. We show that paralogy of RDGN homologs is systemic across arachnopulmonates (arachnid orders that bear book lungs), rather than being a spider-specific phenomenon. A differential gene expression (DGE) analysis comparing the expression of RDGN genes in field-collected embryos of both species identified candidate RDGN genes involved in the formation and reduction of eyes in whip spiders. To ground bioinformatic inference of expression patterns with functional experiments, we interrogated the function of three candidate RDGN genes identified from DGE in a spider, using RNAi in the spider *Parasteatoda tepidariorum*. We provide functional evidence that one of these paralogs, *sine oculis/Six1 A* (*soA*), is necessary for the development of all arachnid eye types. Our results support the conservation of at least one RDGN component across Arthropoda and establish a framework for investigating the role of gene duplications in arachnid eye diversity.

Keywords: cave blindness | *sine oculis* | *Six1* | *Parasteatoda tepidariorum* | Amblypygi | RNAi

Introduction

Cave habitats offer apt systems for investigating the genetic basis of morphological convergence because communities of these habitats are similarly shaped by environmental pressures, such as absence of light and diminished primary productivity (Howarth, 1993; Juan, Guzik, Jaume, & Cooper, 2010). Troglobites, species exclusive to cave environments and adapted to life in the dark, exhibit a suite of characteristics common to cave systems around the world, such as reduction or complete loss of eyes, depigmentation, elongation of appendages and sensory structures, and decreased metabolic activity (Jemec, Škufca, Prevorčnik, Fišer, & Zidar, 2017; Protas & Jeffery, 2012; Riddle et al., 2018). Previous work has shown that troglomorphism can evolve over short time spans (<50 kyr) despite gene flow (Bradic, Teotónio, & Borowsky, 2013; Coghill, Darrin Hulsey, Chaves-Campos, García de Leon, & Johnson, 2014; Herman et al., 2018) and that parallel evolution of troglomorphic traits (e.g., depigmentation; eye loss) in independent populations can involve the same genetic locus (Protas et al., 2005; Protas, Trontelj, & Patel, 2011; Re et al., 2018).

Troglomorphism and troglobitic fauna have been analyzed across numerous taxonomic groups with respect to systematics and population genetics. However, one component of the troglobitic fauna that remains poorly understood is cave arachnids. Most orders of Arachnida are prone to nocturnal life history and some orders broadly exhibit troglophily; in fact, troglobitic species are known from all the extant terrestrial arachnid orders except Solifugae and Uropygi (Cruz-López, Proud, & Pérez-González, 2016; Esposito et al., 2015; Harvey, 2002; 2007; Hedin & Thomas, 2010; Mammola, Mazzuca, Pantini, Isaia, & Arnedo, 2017; Miranda, Aharon, Gavish-Regev, Giupponi, & Wizen, 2016; Santibáñez López, Francke, & Prendini, 2014; Smrž, Kováč, Mikeš, & Lukešová, 2013). In addition to eye and pigment loss, troglomorphism in arachnids manifests in the form of compensatory elongation of walking legs and palps, appendages which harbor sensory structures in this group (Derkarabetian, Steinmann, & Hedin, 2010; Mammola & Isaia, 2017; Mammola et al., 2018a; Mammola, Cardoso, Ribera, Pavlek, & Isaia, 2018b).

Thorough understanding of the developmental genetic basis for the evolution of troglomorphic traits has been largely spearheaded in two model systems: the Mexican cave fish *Astyanax mexicanus* (Bradic et al., 2013; Coghill et al., 2014; Herman et al., 2018; Porter, Dittmar, & Pérez-Losada, 2007; Protas et al., 2005; Protas & Jeffery, 2012) and the cave isopod *Asellus aquaticus* (Jemec et al., 2017; Re et al., 2018; Stahl et al., 2015). Both model systems have more than one hypogean population, can be maintained in laboratories,

77 and are amenable to approaches such as genetic crosses and quantitative trait locus mapping.
78 The advent of short read sequencing technology in tandem with experimental approaches has
79 transformed the potential to triangulate regulatory differences between hypogean
80 (subterranean) and epigean (surface-dwelling) lineages (Protas et al., 2005; Re et al., 2018;
81 Riddle et al., 2018; Stahl et al., 2015), and to study a broader range of cave taxa.
82 Among arthropods, work on the isopod *A. aquaticus* in particular has made significant
83 advances in the identification of loci regulating pigmentation and size of arthropod eyes
84 (Protas et al., 2011; Re et al., 2018), complementing forward and reverse genetic screening
85 approaches in other pancrustacean models (e.g., *Drosophila melanogaster*, *Tribolium*
86 *castaneum*, and *Gryllus bimaculatus*) (Cagan, 2009; Kumar, 2009; Takagi et al., 2012;
87 ZarinKamar et al., 2011). However, developmental and genetic insights into the evolution of
88 blindness illuminated by *A. aquaticus* and other pancrustacean models are not directly
89 transferable to Arachnida for two reasons. First, the eyes of arachnids are structurally and
90 functionally different from those of pancrustaceans. Typically, the main eyes of adult
91 Pancrustacea (e.g., *A. aquaticus*) are a pair of faceted (or apposition) eyes, which are
92 composed of many subunits of ommatidia. In addition, adult Pancrustacea have small median
93 ocelli (typically three in holometabolous insects), often located medially and at the top of the
94 head.
95 By contrast, extant arachnids lack ommatidia and typically have multiple pairs of eyes
96 arranged along the frontal carapace. All arachnid eyes are simple-lens eyes or ocelli; each eye
97 has a single cuticular lens, below which are a vitreous body and visual cells. The retina is
98 composed of the visual cells and pigment cells. These eyes are divided in two types, namely
99 the principal eyes and the secondary eyes (Foelix, 2011; Land, 1985). Principal and
100 secondary eyes differ in the orientation of their retina (Homann, 1971): the principal eyes are
101 of the everted type, with the visual cells lying distally, and lack a reflective layer; the
102 secondary eyes are inverted, with the light-sensitive rhabdomeres pointing away from
103 incoming light (analogous to vertebrate eyes). All secondary eyes possess a reflective layer of
104 crystalline deposits called a tapetum, which is responsible for the "eye shine" of spiders. The
105 principal eyes are the median eyes (ME, also known as anterior medium eyes). The
106 secondary eyes comprise the anterior lateral eyes (ALE), posterior lateral eyes (PLE), and
107 medium lateral eyes (MLE; also known as posterior medium eyes) (Fig. 1A) (Foelix, 2011;
108 Land, 1985) (nomenclature used here follows Schomburg et al 2015). Certain orders and
109 suborders of arachnids have lost one type of eye altogether, with the homology of eyes

110 clarified by the fossil record and embryology (Foelix, 2011; Garwood, Sharma, Dunlop, &
111 Giribet, 2014; Morehouse, Buschbeck, Zurek, Steck, & Porter, 2017).
112 The second concern in extending the model derived from pancrustaceans is that a subset
113 of Arachnida exhibits an ancient shared genome duplication, resulting in numerous paralogs
114 of developmental patterning genes. Recent phylogenetic and comparative genomic works on
115 Arachnida have shown that Arachnopulmonata (Ballesteros & Sharma, 2019; Ballesteros,
116 Santibáñez López, Kováč, Gavish-Regev, & Sharma, 2019; Sharma, Kaluziak, Pérez-Porro,
117 González, Hormiga, et al., 2014a), the clade of arachnids that bear book lungs (e.g., spiders,
118 scorpions, whip spiders), retain duplicates of many key transcription factors, such as
119 homeobox genes, often in conserved syntenic blocks (Leite et al., 2018; Schwager et al.,
120 2017; Sharma, Santiago, González-Santillán, Monod, & Wheeler, 2015a; Sharma, Schwager,
121 Extavour, & Wheeler, 2014b). Many of the ensuing paralogs exhibit non-overlapping
122 expression patterns and a small number have been shown to have subdivided the ancestral
123 gene function (subfunctionalization) or acquired new functions (neofunctionalization) (Leite
124 et al., 2018; Paese, Leite, Schönauer, McGregor, & Russell, 2018; Turetzek, Pechmann,
125 Schomburg, Schneider, & Prpic, 2015).
126 While comparatively little is known about the genetics of arachnid eye development, gene
127 expression surveys of insect retinal determination gene network (RDGN) homologs of two
128 spiders (*Cupiennius salei* and *Parasteatoda tepidariorum*) have shown that this phenomenon
129 extends to the formation of spider eyes as well (Samadi, Schmid, & Eriksson, 2015;
130 Schomburg et al., 2015). Different paralog pairs (orthologs of *Pax6*, *Six1*, *Six3*, *eyes absent*,
131 *atonal*, *dachshund* and *orthodenticle*) exhibit non-overlapping expression boundaries in the
132 developing eye fields, resulting in different combinations of transcription factor expression in
133 the eye pairs (Samadi et al., 2015; Schomburg et al., 2015). While these expression patterns
134 offer a potentially elegant solution to the differentiation of spider eye pairs, only a few
135 studies with the spider *P. tepidariorum* have attempted to experimentally test the role of these
136 genes in the formation of arachnid eyes. *Ptep-orthodenticle-1* maternal RNA interference
137 (RNAi) knockdown results in a range of anterior defects, including complete loss of the head,
138 which precluded assessment of a role in the formation of the eyes (Pechmann, McGregor,
139 Schwager, Feitosa, & Damen, 2009). *Ptep-dac2* RNAi knockdown results in appendage
140 segment defects, but no eye patterning defects were reported by the authors (Turetzek et al.,
141 2015). More recently, a functional interrogation of *Ptep-Six3* paralogs, focused on labrum
142 development, reported no discernible morphological phenotype, despite a lower hatching rate
143 than controls and disruption of a downstream target with a labral expression domain

144 (Schacht, Schomburg, & Bucher, 2020). Thus, gene expression patterns of duplicated RDGN
145 paralogs have never been linked to eye-related phenotypic outcomes in any
146 arachnopulmonate model. Similarly, the functions of the single-copy orthologs of RDGN
147 genes in groups like mites (Grbić et al., 2007; Telford & Thomas, 1998), ticks (Santos et al.,
148 2013), and harvestmen (Garwood et al., 2014; Sharma, Schwager, Giribet, Jockusch, &
149 Extavour, 2013; Sharma, Tarazona, Lopez, Schwager, Cohn, Wheeler, et al., 2015b) are
150 entirely unexplored, in one case because an otherwise tractable arachnid species lacks eyes
151 altogether (the mite *Archegozetes longisetosus* (Barnett & Thomas, 2012; 2013a; 2013b;
152 Telford & Thomas, 1998).
153 Investigating the evolution of eye loss in arachnids thus has the potential to elucidate
154 simultaneously (1) the morphogenesis of a poorly understood subset of metazoan eyes
155 (Foelix, 2011; Morehouse et al., 2017), (2) developmental mechanisms underlying a
156 convergent trait (i.e., eye loss in caves) in phylogenetically distant arthropod groups (Protas
157 & Jeffery, 2012; Re et al., 2018), (3) shared programs in eye development common to
158 Arthropoda (through comparisons with pancrustacean datasets) (Cagan, 2009; Stahl et al.,
159 2015; Takagi et al., 2012; ZarinKamar et al., 2011), and (4) the role of ancient gene
160 duplicates in establishing the diversity of eyes in arachnopulmonates (Leite et al., 2018;
161 Samadi et al., 2015; Schomburg et al., 2015).
162 As first steps toward these goals, we first developed transcriptomic resources for a sister
163 species pair of cave-dwelling *Charinus* whip spiders, wherein one species exhibits typical eye
164 morphology and the other highly reduced eyes (a troglobitic condition). We applied a
165 differential gene expression (DGE) analysis to these datasets to investigate whether candidate
166 RDGN genes with known expression patterns in model spider species (*C. salei*, *P.*
167 *tepidariorum*) exhibit differential expression in non-spider arachnopulmonates, as a function
168 of both eye condition and developmental stage. To link bioinformatic inference of expression
169 patterns with functional outcomes, we interrogated the function of three candidate RDGN
170 genes identified from DGE in a model arachnopulmonate, using RNAi in the spider *P.*
171 *tepidariorum*, which exhibits the same number and types of eyes as whip spiders. We provide
172 functional evidence that one of these candidates, *sine oculis/Six1*, is necessary for the
173 development of all spider eye types.
174
175 **Results**
176
177 *Charinus ioanniticus* and *Charinus israelensis* embryonic transcriptomes

178

179 As an empirical case of closely related, non-spider arachnopulmonate sister species pair
180 that constitutes one epigean and one troglobitic species, we selected the whip spider species
181 *Charinus ioanniticus* and *C. israelensis* (Fig. 1 B–C). Whip spiders, arachnopulmonates of
182 the order Amblypygi, are commonly found in cave habitats ranging from rain forests,
183 savannahs and deserts (Weygoldt, 2000). The recently described troglobitic species *Charinus*
184 *israelensis* (reduced-eyes) occurs in close proximity to its congener *Charinus ioanniticus*
185 (normal-eyes) in caves in the Galilee, northern Israel (Miranda et al. 2016). Given that the
186 formation of Levantine cave refuges is considerably recent, *C. israelensis* and *C. ioanniticus*
187 are likely sister species with a small time of divergence, an inference supported by their
188 similar morphology (Miranda et al 2016). We collected ovigerous females from both species
189 in caves in Israel and extracted RNA from embryos (SI Appendix, Table S1). Embryos of
190 whip-spiders (*Phrynus marginemaculatus*) achieve a deutembryo stage around 20–25 days
191 after egg laying (dAEL), a stage where most external features of the embryo, such as
192 tagmosis and appendages are fully formed, but not the eyes (Weygoldt, 1975). The
193 deutembryo hatches from the egg membrane inside the broodsac carried by the mother, but
194 remains in this stage relatively unchanged for around 70 days. The eyes begin to form around
195 50 dAEL, but the eye spots become externally visible and pigmented only close to hatching
196 (90 dAEL) (Weygoldt, 1975).
197 For *de novo* assembly of the embryonic transcriptomes of *C. ioanniticus* and *C.*
198 *israelensis,* we extracted RNA from all embryonic deutembryo stages collected in the field
199 (see Supplementary Information; table 1 for localities and sample explanations). Assemblies
200 include two deutembryo stages before eyespot formation and one deutembryo stage bearing
201 eyespots for *C. ioanniticus*; and two early deutembryo stages for *C. israelensis* (SI Appendix,
202 Fig. S1).
203 The assembly of *C. ioanniticus* reads resulted in 219,797 transcripts composed of
204 143,282,365 bp with and N50 of 1122 bp (more than 50% of transcripts are 1122 bp or
205 longer) (SI Appendix, Table S2). Universal single copy ortholog benchmarking with BUSCO
206 v3.0 (Waterhouse et al., 2017) indicated 93.8% completeness, with 5.7% of BUSCO genes
207 exhibiting duplication.
208 The assembly *C. israelensis* resulted in a higher number of transcripts: 663,281
209 transcripts composed of 230,044,656 bp and with N50 of 1045 bp. The BUSCO analysis
210 shows 95.2% completeness, which is similar to the value for *C. ioanniticus* assembly.
211

212 RDGN gene duplication in *Charinus* whip spiders
213
214 Amblypygi is inferred to be nested stably in Arachnopulmonata, the clade of arachnids
215 that bear book lungs (Ballesteros & Sharma, 2019; Giribet, 2018; Lozano-Fernandez et al.,
216 2019; Rota-Stabelli et al., 2010; Sharma, Kaluziak, Pérez-Porro, González, Hormiga, et al.,
217 2014a). Recent evidence suggests that the common ancestor of arachnopulmonates has
218 undergone a whole- or partial-genome duplication affecting large gene families, such as
219 homeobox genes (Leite et al., 2018; Schwager et al., 2017; Sharma, Santiago, González-
220 Santillán, Monod, & Wheeler, 2015a). The stable phylogenetic position of Amblypygi in
221 Arachnopulmonata predicts that genes in RDGN that are duplicated in spiders, should also be
222 duplicated in *Charinus* whip spiders. To test this hypothesis, we performed phylogenetically-
223 informed orthology searches on the newly assembled embryonic transcriptomes of both
224 *Charinus* species, and conducted phylogenetic analysis with orthologs across selected
225 arthropod species. We discovered that homologs of *atonal, Pax6*, *dachshund*, *sine oculis*
226 (*Six1*), *Optix* (*Six3*), and *orthodenticle* are duplicated in *Charinus*, whereas *eyegone* and *eyes*
227 *absent* occur as single-copy orthologs (these latter two also occurring single-copy in spiders)
228 (Fig. 2).
229 *atonal*: The *atonal* gene tree showed poor resolution (SI Appendix, Fig. S2), hampering
230 unambiguous assignment of the whip spider genes to *atonal* copies previously annotated in
231 spiders (Samadi et al., 2015; Schwager et al., 2017). *D. melanogaster* copies of *atonal* and
232 *amos* clustered together forming a clade with other pancrustacean and myriapod sequences,
233 suggesting these paralogs are restricted to Mandibulata. The fruit fly *cousin of atonal* (*cato*)
234 formed a clade including the *Cupiennius salei* sequence of *atonalB* whereas the second copy
235 of *C. salei*, *atonalA*, is found in an independent clade with only arachnid sequences. It is in
236 this later clade that the only sequences of *Charinus* related to *atona*l are found, in turn
237 forming two separate clades with clear amino acid differences between these copies (SI
238 Appendix, Dataset S1; *atonal* alignment). Herein, these copies are labeled *atonalA* (*atoA*) and
239 *atonalB* (*atoB*). Note that the reference genomic sequences, annotated as "*atonal like*
240 *homolog 8 like*" (Ptep XP 0159181091), is found orthologous to the gene *net* in *D.*
241 *melanogaster*.
242 *Pax6*: In *D. melanogaster*, there are two paralogous copies of the vertebrate *Pax6*, *eyeless*
243 and *twin of eyeless*. This duplication seems to be shared across all arthropods and both *Pax6*
244 copies have been characterized in spiders (Samadi et al., 2015; Schomburg et al., 2015). The
245 gene tree of *Pax6* homologues clearly identified a clade for *toy* including chelicerate and

246 mandibulate copies, but no *Charinus* sequences are found in this clade (SI Appendix, Fig.
247 S3). The sister clade (*eyeless*) consists only of pancrustacean sequences whereas the
248 chelicerate copies, previously annotated as *eyeless* orthologs, are found in a separate clade.
249 Among these, two distinct genes, herein dubbed *Pax6A* and *Pax6B*, are present in both
250 *Charinus* species. Sequence similarity searches (blastp) of both *Pax6A* and *Pax6B* against the
251 genome of *Drosophila melanogaster* points to *Dmel-toy* as the best hit, followed by *Dmel-ey*.
252 Therefore, although the homology of these copies with *Dmel-ey/toy* is evident, it is not trivial
253 to assign these to either of these genes or if these represent taxon-restricted duplicates of
254 *eyeless*.
255 *eyegone/twin of eyegone*: These members of the Pax gene family are paralogous in *D.*
256 *melanogaster* but occur as single copy in arachnids. Single copy orthologs of eyg/toe are
257 present in the two target Amblypygi species (SI Appendix, Fig. S3).
258 *dachshund*: Spiders and scorpions have two paralogous copies of *dachshund* (Nolan,
259 Santibáñez López, & Sharma, 2020; Turetzek et al., 2015). Two copies are present in the
260 transcriptomes of both *Charinus* species and are here termed *dacA* and *dacB* (SI Appendix,
261 Fig. S4). The *C. israelensis dacB* is assembled in two different gene fragments that overlap
262 by three amino acids (SI Appendix, Fig. S4; see *dachshund* alignment in SI Appendix
263 Dataset S1). The *C. ioanniticus dacA* copy is also assembled as two different gene fragments
264 with little sequence overlap but being part of the *dacA* clade (SI Appendix, Fig. S4).
265 *eyes absent*: This single-copy orthologs are found in arthropods and arachnids alike
266 and is represented in both *Charinus* species. The association of transcript to this gene is
267 unambiguous for both amblypigid species (SI Appendix, Fig. S5).
268 *orthodenticle*: As with spiders, there are two copies homologous to *Dmel-otd* in
269 *Charinus*. The resolution of the gene tree is poor and does not allow uncontroversial
270 association to spider orthologs (SI Appendix, Fig. S6). *Charinus* copies are termed *otdA* and
271 *otdB*.
272 *Optix*: There are two very similar copies of *Optix* in *C. israelensis* and one in *C.*
273 *ioanniticus* (SI Appendix, Fig. S7). The *C. ioanniticus* copy is termed *OptixA*. The two copies
274 of *C. israelensis* show very conserved amino acid sequences but clear nucleotide differences.
275 Although the gene tree with the reference genome shows them more closely allied to one of
276 the spider paralogous copies of *Optix* (Ptep NP 00130752.1), a reduced analysis including
277 *Cupiennius salei* and *P. tepidariorum* copies, suggests that the *Charinus* copies are
278 independent duplications. Here the two whip spider copies are dubbed *OptixA* and *OptixB* but
279 they should not be considered orthologous to the spider *OptixA/B*.

280 *sine oculis:* Two copies of *sine oculis* are found in *C. israelensis* and one in *C.*
281 *ioanniticus*. Both copies are nested in a clade with *Ptep-soA* (SI Appendix, Fig. S8). These
282 are herein dubbed as *soA* and *soB* given that orthology with either spider copy is unclear.
283
284 RDGN genes in whip spider eye formation: comparing early and late stages of *C. ioanniticus*
285
286 The expression of paralog pairs of *Pax6*, *sine oculis*, *Optix*, *eyes absent*, *atonal*,
287 *dachshund* and *orthodenticle* in the developing eyes of the spiders (Samadi et al., 2015;
288 Schomburg et al., 2015), and the occurrence of the same paralogs in *Charinus* whip spiders,
289 suggest that these genes may also be involved in the formation of eyes in whip spiders. We
290 investigated this idea by comparing the expression levels of these RDGN genes in the stages
291 before eye-spot formation versus a stage after eye-spot formation in the eye-bearing whip
292 spider *Charinus ioanniticus* (henceforth "Comparison 1"; Fig. 3A).
293 We mapped reads of both treatments to the reference transcriptome of *C. ioanniticus*
294 using the quasi-alignment software Salmon v. 1.1.0 (Patro, Duggal, Love, Irizarry, &
295 Kingsford, 2017) and conducted a differential gene expression analysis of Comparison 1
296 using DESeq2 v 1.24.0 (Love, Huber, & Anders, 2014) (SI Appendix, Fig. S9). These
297 comparisons showed that *Cioa-dacA*, *Cioa-otdA*, *Ciao-eya* and *Cioa-soA* are significantly
298 over-expressed ($p_{adj} < 0.05$) in the eyespot stage in comparison with the stage before eyespot
299 formation (Fig. 3A). While we cannot rule out that the differences in gene expression are due
300 to other developmental differences between the two stages sequenced, these results
301 highlighted these four RDGN genes as promising candidates involved in the formation of
302 eyes in whip spiders.
303
304 RDGN genes in whip spider eye reduction: comparing *C. ioanniticus* and *C. israelensis*
305
306 Blindness in adults of the model cave fish *Astyanax mexicanus* is a result of an embryonic
307 process in which the rudimentary eye of the embryo is induced to degenerate by signals
308 emitted from the lens tissue (Jeffery, 2009). Both early and late expression of RDGN genes,
309 such as Pax6, are responsible for the reduction of eyes in fish from cave populations
310 (Jeffery, 2009; Strickler, Yamamoto, & Jeffery, 2001). Likewise, in the isopod crustacean
311 *Asellus aquaticus* cave blindness has a strong genetic component and mechanisms of eye
312 reduction also act at embryonic stages (Mojaddidi, Fernandez, Erickson, & Protas, 2018;
313 Protas et al., 2011). The embryonic development of the reduced-eyes whip spider *C.*

314 *israelensis* has not been explored to date, but we expect that reduction of eyes results from
315 changes in embryonic gene expression during the deutembryo stage (Weygoldt, 1975). We
316 investigated this possibility by quantifying the relative gene expression of RDGN genes in
317 comparable embryonic stages of *C. israelensis* (reduced eyes) and *C. ioanniticus* (normal
318 eyes) embryos before eye-spot formation (SI Appendix Table S1; Figure S1). Using the DGE
319 approach from Comparison 1, we conducted a heterospecific analysis using as the reference
320 either the *C. israelensis* transcriptome (henceforth "Comparison 2.1") or the *C. ioanniticus*
321 transcriptome (henceforth "Comparison 2.2").
322 Both analyses are anchored on the premise that a hybrid mapping between the sister
323 species is possible given the recent divergence between them. The mapping rate of the *C.*
324 *ioanniticus* reads was similar regardless of the reference species, (96.74% and 96.59%
325 respectively for *C. ioanniticus* and *C. israelensis*). In the case of the reads from *C. israelensis*
326 embryos, mapping rate to the conspecific (96.8%) transcriptome was higher than when
327 mapping against *C. ioanniticus* (82.45%). The similar mapping rate of *C. ioanniticus* reads
328 suggests that the two whip spiders are sufficiently closely related to generate interspecific
329 comparisons of gene expression. Comparisons 2.1 and 2.2 yielded similar results with respect
330 to the direction of differentially expressed RDGN genes (Fig. 3B–C). In comparison 2.1,
331 *Pax6A*, *OptixA* and *OptixB* are significantly over-expressed in the normal-eyes species, with
332 expression levels at least 4 times higher than in the reduced-eyes species ($\log_2 FC > 2$; $p_{adj} <$
333 0.05) (Fig. 3B; SI Appendix, Fig. S10). In comparison 2.2, *Pax6A* and *OptixA* are also over-
334 expressed in *C. ioanniticus* ($p_{adj} < 0.05$), and so is *eyes absent* ($p_{adj} < 0.05$; Fig. 3C). In
335 comparison 2.2, *orthodenticle-B* appears under-expressed in the normal-eyes species ($p_{adj} <$
336 0.05 (Fig. 3C; SI Appendix, Fig. S11). We note that the magnitude of $\log_2 FC$ and
337 significance values differed considerably between analysis. Nonetheless, *Pax6A* and *OptixA*
338 were consistently over expressed in the normal-eyes species, highlighting these two genes as
339 promising candidates involved in the reduction of eyes in *Charinus israelesis*.
340
341 *sine oculis* is necessary for principal and secondary eye development in a model
342 arachnopulmonate
343
344 Our bioinformatic analysis in the whip spider system suggested that *eyes absent* and
345 paralogs of *sine oculis*, *orthodenticle*, and *dachshund* may be involved in the normal
346 formation of eyes in *C. ioanniticus* (Comparison 1). We also found evidence that *Pax6* and a
347 paralog of *Optix* may be involved in the reduction of eyes in the cave whip spider *C.*

348 *israelensis*. To link bioinformatic reconstructions of gene expression with functional
349 outcomes, we interrogated the function of RDGN genes using parental RNA interference
350 (RNAi) in the spider *Parasteatoda tepidariorum*. We selected *Ptep-soA* (*Ptep-so1 sensu*
351 Schomburg et al. 2015)*, Ptep-otdB* (*Ptep-otd2 sensu* Schomburg et al. 2015) and *Ptep-OptixB*
352 (*Ptep Six3.2 sensu* Schomburg et al. 2015). In *P. tepidariorum*, these genes are known to be
353 expressed in all eye types, in the median eyes only, and in the lateral eyes, respectively (Fig.
354 1D) (Schomburg et al., 2015).
355 Early expression of *Ptep-soA* is detected in lateral domains of the head lobes (stage 10)
356 corresponding to the principal and secondary eyes, and continues until the pre-hatching stage
357 14 (Schomburg et al., 2015). Expression of *Ptep-soA* on wild type stage 14.1 embryos is
358 bilaterally symmetrical on all eyes and uniformly strong (Fig. 4A–B). By stage 14.2, it
359 remains strong on the principal eyes but it is stronger at the periphery of the secondary eye
360 spots (Fig. 4A, C).
361 *P. tepidariorum* hatchlings, or postembryos, initially have no externally visible lenses and
362 pigment. The red pigment and lenses of all eyes, and the reflective tapetum of the lateral
363 eyes, become progressively recognizable in the 48 hours (at 26˚C) until the animal molts into
364 the first instar with fully formed eyes (SI Appendix, Video S1) (see also Mittmann & Wolff,
365 2012). We fixed embryos from *Ptep-soA* dsRNA-injected and dH2O-injected treatments
366 between 24h-48h, which encompasses stages where the eyes of postembryos are already
367 recognizable until the first instar.
368 Negative control experiments (dH_2O-injected females) yielded postembryos with eye
369 morphology indistinguishable from wild type animals: the median eyes (ME; principal eyes)
370 have an inferior semi-lunar ring of red pigment and lack the tapetum; and all pairs of lateral
371 eyes (secondary eyes) have the canoe-shaped tapetum type (Foelix, 2011; Land, 1985), which
372 is split in the middle and surrounded by red pigment (Fig. 5A; panel 1). We observed
373 misshaped tapeta on the lateral eyes of some postembryos on the earlier side of the
374 developmental spectrum of fixed animals, but that was never observed on postembryos close
375 to molting or first instars (SI Appendix, Fig. S12). It is unclear if this reflects a natural
376 variation of early developing tapetum or an artifact of sample preparation.
377 Embryos from *Ptep-soA* dsRNA-injected females are also able to hatch into postembryos
378 and continue molting to adulthood (SI Appendix, Video S2). However, a subset of the
379 embryos of dsRNA-injected treatment (9.5%; n=195/2049) exhibits a spectrum of eye defects
380 that was not observed on the controls (Fig. 5A–B; SI Appendix, Fig. S13). The defects
381 occurred on all eyes, namely medium eyes (ME), anterior lateral eyes (ALE), posterior lateral

382 eyes (PLE), and medium lateral eyes (MLE) (Fig. 5A). Affected medium eyes have reduced
383 pigmentation or complete absence (Fig. 5A, panels 2–6), while lateral eyes also exhibited
384 defects of the tapetum or complete absence of the eye (Fig. 5A, panels 4–6).
385 We selected a subset of the knockdown postembryos initially scored as having any eye
386 defect (n=48) for quantifying the degree of effect per eye type, and the proportion of
387 symmetrical and mosaic eye phenotypes in our sample. Medium eyes are affected in almost
388 all cases (97%), whereas the three lateral eye types were similarly lowly affected (MLE:
389 14%; PLE: 8%; ALE: 10%) (Fig. 5C; SI Appendix, Fig. S12; detailed scoring criteria in
390 Material and Methods). The majority of defective eyes are mosaics, meaning that a given eye
391 pair is affected only on one side of the animal (Fig. 5C; SI Appendix, Fig. S12).
392 Parental RNAi against *Ptep-soA* did not completely abolish its expression, as detected by
393 in situ hybridization (Fig. 4D; see Material and Methods). Nevertheless, we detected
394 asymmetrical reduction of *Ptep-soA* expression on single eyes of a subset of stage 14
395 embryos (n=6/16; Fig. 4D), which closely correlates with the predominance of mosaic
396 phenotypes observed in late postembryos (Fig. 5C).
397 Parental RNAi experiments using the same protocol targeting *Ptep-otdB* and *Ptep-OptixB*
398 did not result in any detectable phenotypic effects on the eyes of embryos from dsRNA-
399 injected treatment (two and six females injected, respectively; counts not shown). These
400 results accord with a recent study that knocked down both *Optix* paralogs *P. tepidariorum*
401 and did not recover eye defects (Schacht et al., 2020)
402
403 **Discussion**
404
405 Paralogy of RDGN members in arachnopulmonates
406
407 Amblypygi have a critical placement within arachnid phylogeny, as they are part of a trio
408 of arachnid orders (collectively, the Pedipalpi, comprised of Amblypygi, Thelyphonida, and
409 Schizomida), which in turn is the sister group to spiders. Whereas the eyes of spiders have
410 greatly diversified in structure, function, and degree of visual acuity (particularly the eyes of
411 hunting and jumping spiders), the arrangement and number of eyes in Amblypygi likely
412 reflects the ancestral condition across Tetrapulmonata (= spiders + Pedipalpi), consisting of
413 three pairs of simple lateral ocelli and a pair of median ocelli; a similar condition is observed
414 in basally branching spider groups like Mesothelae and Mygalomorphae, as well as
415 Thelyphonida (vinegaroons). However, while developmental genetic datasets and diverse

416 genomic resources are available for spiders and scorpions (Oda & Akiyama-Oda, 2020;
417 Posnien et al., 2014; Schwager et al., 2017; Sharma, Schwager, Extavour, & Wheeler,
418 2014b), the developmental biology of the other three arachnopulmonate orders has been
419 virtually unexplored in the past four decades beyond a single work describing the
420 embryology of one North American amblypygid species (Weygoldt, 1975). To address this
421 gap, we focused our investigation on a sister species pair of cave whip spiders and generated
422 the first embryonic transcriptomes for this order. These datasets are immediately amenable to
423 testing the incidence of RDGN duplicates previously known only from two spiders (Samadi
424 et al., 2015; Schomburg et al., 2015) and their putative effects in patterning eyes across
425 Arachnopulmonata broadly.
426 The inference of a partial or whole genome duplication (WGD) in the most recent
427 common ancestor of Arachnopulmonata is supported by the systemic duplications of
428 transcription factors and synteny detected in the genomes of the scorpion *Centruroides*
429 *sculpturatus,* and the spider *Parasteatoda tepidariorum*, as well as homeobox gene
430 duplications detected in the genome of the scorpion *Mesobuthus martensii* and transcriptome
431 of the spider *Pholcus phalangioides* (Leite et al., 2018; Schwager et al., 2017). Additional
432 evidence comes from shared expression patterns of leg gap gene paralogs in a spider and a
433 scorpion (Nolan et al., 2020). Embryonic transcriptomes are particularly helpful in the
434 absence of genomes, as several duplicated genes, such as some homeobox genes, are only
435 expressed during early stages of development (Leite et al., 2018; Sharma, Santiago,
436 González-Santillán, Monod, & Wheeler, 2015a; Sharma, Schwager, Extavour, & Wheeler,
437 2014b). Our analysis of *Charinus* embryonic transcriptomes shows that RDGN gene
438 duplicates observed in spiders also occur in whip spiders, supporting the hypothesis that these
439 paralogous copies originated from a shared WGD event in the common ancestor of
440 Arachnopulmonata.
441 The conservation of some transcription factors patterning eyes is widespread in the
442 Metazoan tree of life (Vopalensky & Kozmik, 2009). In the model fruit fly *D. melanogaster*,
443 the homeobox Pax6 homolog, *eyeless*, was the first transcription factor identified as a "master
444 gene", necessary for compound eye formation and capable of inducing ectopic eye formation
445 (Gehring & Ikeo, 1999; Kumar, 2009). The Pax6 protein is essential for eye formation across
446 several metazoan taxa, which has fomented ample debate about the deep homology of gene
447 regulatory networks in patterning structurally disparate eyes (Carroll, 2008; Shubin, Tabin, &
448 Carroll, 2009; Vopalensky & Kozmik, 2009). In the case of *sine oculis* (Six1/2), orthologs
449 are found across metazoans (Bebenek, Gates, Morris, Hartenstein, & Jacobs, 2004; Byrne et

450 al., 2017; Rivera et al., 2013). Evidence that *sine oculis* is required for the eye patterning in
451 other bilaterians comes from expression pattern in the developing eyes of the annelid
452 *Platynereis dumerilii* (Arendt, Tessmar, Medeiros de Campos-Baptista, Dorresteijn, &
453 Wittbrodt, 2002), and functional experiments in the planarian *Girardia tigrina* (Pineda et al.,
454 2000). Therefore, studies interrogating the genetic bases of eye formation in chelicerate
455 models have the potential to clarify which components of the eye gene regulatory network of
456 Arthropoda evolved in the MRCA of the phylum, and which reflect deep homologies with
457 other metazoan genes.
458
459 A conserved role for a *sine oculis* homolog in patterning arachnopulmonate eyes
460
461 The eyes of arthropods are diverse in number, arrangement, structure and function
462 (Paulus, 1979). Both types of eyes observed in Arthropoda, the faceted eyes (compound) and
463 single-lens eyes (ocelli), achieve complexity and visual acuity in various ways. To mention
464 two extremes, in Mandibulata the compound eyes of mantis shrimps (Stomatopoda) achieve a
465 unique type of color vision and movements by using 12 different photoreceptive types and
466 flexible eye-stalks (Daly, How, Partridge, & Roberts, 2018; Marshall, Cronin, & Kleinlogel,
467 2007; Thoen, How, Chiou, & Marshall, 2014). In Arachnida, the simple-lens median eyes of
468 some jumping spiders (Salticidae) have exceptional visual acuity in relation to their eye size,
469 achieve trichromatic vision through spectral filtering, and can move their retina using
470 specialized muscles (Harland, Li, & Jackson, 2012; Land, 1985; Zurek et al., 2015).
471 Comparative anatomy suggests that the common ancestor of Arthropoda had both lateral
472 compound eyes and median ocelli that then became independently modified in the arthropod
473 subphyla (Morehouse et al., 2017; Paulus, 1979). While in situ hybridization data for selected
474 RDGN genes across arthropods generally support the hypotheses of eye homology,
475 comparative developmental datasets remain phylogenetically sparse outside of Pancrustacea
476 (Samadi et al., 2015; Schomburg et al., 2015)
477 We therefore applied a bioinformatic approach in a study system that lacked any genomic
478 resources (Amblypygi) to assess whether RDGN homologs are transcriptionally active during
479 the formation of eyes in the eye-bearing *C. ioanniticus* (Comparison 1), as well as those that
480 may be putatively involved in eye loss in its troglobitic sister species (Comparison 2). As first
481 steps toward understanding how arachnid eyes are patterned, our experiments demonstrated
482 that *soA*, a *sine oculis* paralog identified as differentially expressed during the formation of
483 eyes in *C. ioanniticus*, is necessary for patterning all eyes of a model arachnid system with

484 the same eye configuration (*Parasteatoda tepidariorum*). Thus, we provide the first
485 functional evidence that part of the RDGN is evolutionarily conserved in the most recent
486 common ancestor (MRCA) of insects and arachnids, and by extension, across Arthropoda.
487 The advantage of such a bioinformatic approach is that it can potentially narrow the range
488 of candidate genes for functional screens, due to the inherent challenges imposed by paralogy
489 when assessing gene function. Eye reduction in the cave fish *Astyanax mexicanus* has been
490 shown to involve differential expression of genes known to be involved in eye patterning in
491 model organisms, such as *hedgehog* and *Pax6* (*eyeless/toy*) (Jeffery, 2009; Protas & Jeffery,
492 2012). In addition, other "non-traditional" candidates have been identified, such as *hsp90*
493 (Jeffery, 2009). Likewise, evidence from quantitative trait loci mapping in cave populations
494 of the troglobitic crustacean *Asellus aquaticus* shows that eye loss phenotype is correlated
495 with loci that are not part of the RDGN (Protas et al., 2011; Protas & Jeffery, 2012). The
496 results of the DGE analysis in whip spiders underscore the potential of a DGE approach to
497 triangulate targets among candidate genes in non-model species more broadly. Future efforts
498 in the *Charinus* system should focus on dissecting individual eye and limb primordia of
499 embryos of both species, in order to identify candidate genes putatively involved in the
500 reduction of each eye type, as well as compensatory elongation of the sensory legs of the
501 troglobitic species, toward downstream functional investigation.
502
503 Do gene duplications play a role in the functional diversification of arachnopulmonate eyes?
504
505 A challenge in studying arachnopulmonate models to understand ancestral modes of eye
506 patterning in Arthropoda is the occurrence of RDGN duplicates in this lineage. Our orthology
507 searches and phylogenetic analysis showed that the evolutionary history of genes is not
508 always resolved using standard phylogenetic methods, as short alignable regions and/or
509 uncertainty of multiple sequence alignments can result in ambiguous gene trees. One way to
510 circumvent this limitation is by analyzing expression patterns via in situ hybridization
511 between paralogs in different arachnids in order to determine which patterns are
512 plesiomorphic (Leite et al., 2018; Nolan et al., 2020; Turetzek et al., 2015). Nonetheless, the
513 possibility of subfunctionalization and neofunctionalization may also complicate such
514 inferences because discerning one process from the other is analytically challenging (Sandve,
515 Rohlfs, & Hvidsten, 2018).
516 Genetic compensation of gene paralogs is another confounding variable, which can be
517 accounted for by experimental advances in model organisms (e.g., Shull et al., 2020). We

518 note that the overall penetrance in this experiment is low (9.5%) when compared to some
519 studies in *P. tepidariorum* (e.g., Khadjeh et al 2012; >59% in *Ptep-Antp* RNAi). Wide
520 variance in penetrance has been reported by several research groups in this system, with
521 phenotypic effects varying broadly even within individual experiments (e.g., Fig. 5 of
522 Akiyama-Oda & Oda, 2006; Fig. S5 of Schwager, Pechmann, Feitosa, McGregor, & Damen,
523 2009). Furthermore, some genes have empirically proven intractable to misexpression by
524 RNAi in *P. tepidariorum*, with one case suggesting functional redundancy of posterior Hox
525 genes to be the cause (Khadjeh et al., 2012). Double knockdown experiments have been
526 shown to exhibit poor penetrance (0-1.5%) in *P. tepidariorum* as well (Fig. S3 of Khadjeh et
527 al. 2012; Fig. S1 of Setton et al., 2017), and to our knowledge, no triple knockdown has ever
528 been achieved. While we cannot rule out functional redundancy with other RDGN paralogs
529 in the present study, the low penetrance we observed may also be partly attributable to our
530 conservative phenotyping strategy (see Material and Methods), which did not assess a
531 possible delay in eye formation and emphasized dramatic defects in eye morphology for
532 scoring.
533 The occurrence of RDGN gene duplications in Arachnopulmonata, in tandem with
534 improving functional genetic toolkits in *P. tepidariorum* (e.g., Pechmann, 2016), offers a
535 unique opportunity of studying the role of sub- and neofunctionalization in the development
536 of their eyes, and a possible role of this process in the diversification of number, position and
537 structure of the eyes in an ancient group of arthropods (Harland et al., 2012; Land, 1985;
538 Morehouse et al., 2017; Paulus, 1979; Zurek et al., 2015). The genomes of mites, ticks, and
539 harvestmen (Grbić et al., 2011; Hoy et al., 2016) (Gulia-Nuss et al., 2016) reveal that
540 apulmonate arachnid orders have not undergone genome duplication events as seen in
541 Arachnopulmonata (Schwager et al., 2017), or horseshoe crabs (Kenny et al., 2015; Nossa et
542 al., 2014; Zhou et al., 2020). Future comparative studies focused on understanding the
543 ancestral role of chelicerate RDGN genes should additionally prioritize single-copy orthologs
544 in emerging model systems independent of the arachnopulmonate gene expansion, such as
545 the harvestman *Phalangium opilio* (Sharma et al., 2013; Sharma, Schwager, Extavour, &
546 Giribet, 2012).
547
548 **Materials and Methods**
549
550 Animal collection
551

552 Three ovigerous females of the normal-eyes species, *Charinus ioanniticus* (ISR021-2;
553 ISR021-3; ISR021-4), and two egg-carrying females of the reduced-eyes species, *Charinus*
554 *israelensis* (ISR051-4; ISR051-6), were hand collected in caves in Israel in August 2018
555 (Supplementary Information; Table 1). Females were sacrificed and the brood sacs
556 containing the embryos were dissected under phosphate saline buffer (PBS). For each female,
557 a subset of the embryos (5 to 13 individuals) was fixed in RNAlater solution after poking a
558 whole into the egg membrane with fine forceps, while the remaining embryos of the clutch
559 were fixed in a 4% formaldehyde/PBS solution to serve as vouchers (SI Appendix, Table S1).
560 Adult animals and embryos of *Parasteatoda tepidariorum* were obtained from the colony at
561 UW-Madison, US.
562
563 Transcriptome assembly for *Charinus* whip spiders
564
565 RNAlater-fixed embryos were transferred to 1.5mL tubes filled with TRIZOL
566 (Invitrogen) after two months, and subject to RNA extraction. Total RNA extracted from
567 each sample of the embryos of *C. ioannicitus* (three samples) and *C. israelensis* (two
568 samples) (SI Appendix, Table S1) was submitted for library preparation at the Biotechnology
569 Center of the University of Wisconsin-Madison. Each sample was sequenced in triplicate in
570 an Illumina High-Seq platform using paired-end 100 bp-long read strategy at the same
571 facility. Read quality was assessed with FastQC (Babraham Bioinformatics). Paired-end
572 reads for *C. ioanniticus* (ISR021) and *C. israelensis* (ISR051) were compiled and *de novo*
573 assembled using Trinity v.3.3 (Grabherr et al., 2011) enabling Trimmomatic v.0.36 to remove
574 adapters and low-quality reads (Bolger, Lohse, & Usadel, 2014). Transcriptome quality was
575 assessed with the Trinity package script '*TrinityStats.pl*' and BUSCO v.3 (Waterhouse et al.,
576 2017). For BUSCO, we used the 'Arthropoda' database and analyzed the transcriptomes
577 filtered for the longest isoform per Trinity gene.
578
579 RNA sequencing for differential gene expression
580
581 The total RNA extraction of each sample of *C. ioanniticu*s and *C. israelensis* embryos
582 was sequenced in triplicate in an Illumina High-Seq platform using a single-end 100 bp-long
583 read strategy in the same facility as described above. For *C. ioanniticus* (normal-eyes), we
584 sequenced two biological replicates of embryos at an early embryonic stage, before eye-spot
585 formation (ISR021-2, ISR021-3), and one sample of late embryos, after eye-spot formation

586 (ISR021-4); For *C. israelensis* (reduced-eyes), we sequenced embryos at an early embryonic
587 stage (ISR051-6; ISR051-4) comparable to the early stage in *C. ioanniticu*s (ISR021-2,
588 ISR021-3), as inferred by the elongated lateral profile of the body and marked furrows on the
589 opisthosomal segments (SI Appendix, Fig. S1).
590
591 Differential gene expression analysis in *Charinus* and identification of eye gene orthologs
592
593 Orthologs of *Drosophila melanogaster eyeless* and *twin of eyeless* (*Pax6A, Pax6B*), *sine*
594 *oculis* (*soA*, *soB*), *orthodenticle* (*otdA*, *otdB*), *Optix* (*Six3.1*, *Six3.2*), *dachshund* (*dacA*, *dacB*),
595 and *eyes absent* (*eya*) had been previously isolated in *Parasteatoda tepidariorum*
596 (Schomburg et al., 2015, and references therein). We used as reference sequences the
597 complete predicted transcripts for these genes from *P. tepidariorum* genome (Schwager et al.,
598 2017), *Cupiennius salei* (Samadi et al., 2015) (for *atonal* and *Pax6*), and *D. melanogaster*,
599 including also *atonal* and *eyegone* from the latter species. The sequences were aligned with
600 MAFFT (v7.407) (Katoh & Standley, 2013) and the resulting alignment used to build hidden
601 Markov model profiles for each gene (hmmbuild, from the hmmer suite v.3.3) (Finn et al.,
602 2015). Matches to these profiles were found using hmmsearch in the reference transcriptomes
603 of *C. ioanniticus* and *C. israelensis* as well as in the genomes of representative arthropods
604 including *D. melanogaster* (GCA 000001215.4), *Tribolium castaneum* (GCA 000002335.3),
605 *Daphnia magna* (GCA 003990815.1), *Strigamia maritima* (GCA 000239455.1),
606 *Dinothrombium tinctorium* (GCA 003675995.1), *Ixodes scapularis* (GCA 002892825.2),
607 *Tetranychus urticae* (GCA 000239435.1), *Limulus polyphemus* (GCA 000517525.1),
608 *Tachypleus tridentatus* (GCA 004210375.1), *Centruroides sculpturatus* (GCA 000671375.2),
609 *Parasteatoda tepidariorum* (GCA 000365465.2) and *Trichonephila clavipes* (GCA
610 002102615.1). These species were selected from a pool relatively recent genome assembly
611 resources and well curated reference genomes.
612 Homologous sequences (those with hmmer expectation value, $e < 10^{10}$) to the genes of
613 interest were then compiled into individual gene FASTA files, combined with the reference
614 sequences used for the homology search, aligned (MAFFT), trimmed of gap rich regions
615 (trimAL v.1.2 , –gappyout) (Capella-Gutiérrez, Silla-Martínez, & Gabaldón, 2009) and used
616 for maximum likelihood gene tree estimation (IQTREE v.1.6.8, –mset
617 LG,WAG,JTT,DCMUT –bb 1000) (Nguyen, Schmidt, Haeseler, & Minh, 2015). The
618 association of transcripts in the *Charinus* species with the genes of interest is based on the
619 gene phylogeny and was followed by inspection of the coding sequences to distinguish

splicing variants from other gene copies. Alignments and the list of *Charinus* sequences is available in SI Appendix Dataset S1. These gene transcript association was then used for the transcript to gene map required for the DGE analysis.

Read mapping, transcript abundance quantification

For the *in-silico* analysis of gene expression, single-end raw reads were first trimmed using the software Trimmomatic v. 0.35 (Bolger et al., 2014). For the intra-specific analysis of early (before eyespot) and late (eyespot) embryos of *C. ioanniticus* (Comparison 1), the trimmed reads were quantified in the embryonic transcriptome of *C. ioanniticus*. For the intra-specific comparison of early embryos of *C. ioanniticus* and *C. israelensis*, two reciprocal analysis were conducted: reads from both species mapped onto *C. israelensis* transcriptome as the reference (Comparison 2.1); and reads from both species mapped onto *C. ioanniticus* transcriptome (Comparison 2.2).

Transcript abundance was quantified using the software Salmon v. 1.1.0 (Patro et al., 2017), enabling '*–validateMapping*' flag. Analysis of differential gene expression was conducted with the software DESeq2 v 1.24.0 (Love et al., 2014) following a pipeline with the R package *tximport* v.1.12.3 (Soneson, Love, & Robinson, 2015). The exact procedures are documented in the custom R script (SI Appendix, Dataset S2)

Parental RNA interference, in situ hybridization, and imaging in *Parasteatoda tepidariorum*

Total RNA from a range of embryonic stages of *P. tepidariorum* was extracted with TRIZOL (Invitrogen), and cDNA was synthetized using SuperScriptIII (Invitrogen). Gene fragments for *Ptep-sine oculis A* (*soA*), *orthodenticle B* (*otdB*) and *OptixB* were amplified from cDNA using gene specific primers designed with Primers3Web version 4.1.0 (Koressaar & Remm, 2007) and appended with T7 ends. Cloning amplicons were generated using the TOPO TA Cloning Kit with One Shot Top10 chemically competent *Escherichia coli* (Invitrogen). Amplicon identities and directionality were assessed with Sanger sequencing. Primer, amplicon sequences and fragment lengths are available in SI Appendix Dataset S3. Double-stranded RNA for *Ptep-soA*, *Ptep-otdB* and *Ptep-OptixB* was synthetized from amplicon on plasmids using MEGAScript T7 transcription kit (Thermo Fischer) with T7/T7T3 primers. Sense and antisense RNA probes for colorimetric in situ hybridization

653 were synthetized from plasmid templates with DIG RNA labeling mix (Roche) and T7/T3
654 RNA polymerase (New England Biolabs) using the manufacturer's instructions.
655 Parental RNA interference (RNAi) followed established protocols for double-stranded
656 RNA (dsRNA) injection in virgin females of *P. tepidariorum* (Oda & Akiyama-Oda, 2020).
657 Each female was injected four times with 2.5 µL of dsRNA at a concentration of 2 µg/uL, to
658 a total of 20µg. For *Ptep-soA*, seven virgin females were injected with dsRNA of a 1048bp
659 cloned fragment (SI Appendix, Fig. S13C) and 3 females were injected with the same volume
660 of dH_2O as a procedural control. Two virgin females were injected with dsRNA for *Ptep-*
661 *otdB*, and six females for *Ptep-OptixB*. All females were mated after the second injection, and
662 were fed approximately every-other day after the last injection. Cocoons were collected until
663 the sixth clutch, approximately one per week.
664 Hatchlings for all cocoons were fixed between 24–48 hours after hatching. Freshly
665 hatched postembryos have almost no external signs of eye lenses and pigments. The selected
666 fixation window encompasses a period in which postembryos have deposited eye pigments
667 until the beginning of the first instar, where eyes are completely formed (SI Appendix, Video
668 S1, S2). Hatchlings were immersed in 25% ethanol/PBST and stored at 4ºC. For the *Ptep-soA*
669 RNAi experiment, hatchlings were scored in four classes: (1) wild type, where all eyes were
670 present and bilaterally symmetrical; (2) Eyes defective, where one or more eyes were reduced
671 in size or completely absent; (3) dead/arrested; (4) Undetermined, where embryos were
672 damaged or clearly freshly hatched. A subset of *Ptep-soA* dsRNA-injected embryos from four
673 clutches (n=48) and of three control clutches (n=48) were further inspected in detail to assess
674 the effects on individual eye types. Given that there is a spectrum on the intensity of pigment
675 deposition in the medium eyes (ME), and small asymmetries on the shape of the early
676 developing tapetum of the lateral eyes (LE) in control embryos, the following conservative
677 criteria was adopted: ME were considered affected when asymmetry in pigmentation or lens
678 size was detected. Both ME were only scored as affected when they were both completely
679 missing, in order to rule out embryos were simply delayed in pigment deposition; LE were
680 considered defective only when the tapetum was completely absent (SI Appendix, Fig. S12).
681 Therefore, our coding does not allow detection of a phenotype consisting of delayed
682 pigmentation.
683 For in situ hybridization, a subset of *Ptep-soA* dsRNA-injected embryos at stage 13/14
684 (Mittmann & Wolff, 2012) was fixed in a phase of heptane and 4% formaldehyde for 12–24
685 hours, washed in PBST, gradually dehydrated in methanol and stored at -20ºC for at least 3

days before downstream procedures, after a modified protocol of Akiyama-Oda and Oda (2003). In situ hybridization followed the protocol of Akiyama-Oda and Oda (2003).

Embryos from in situ hybridization were stained with Hoechst nuclear staining and imaged in a Nikon SMZ25 fluorescence stereomicroscope mounted with a DS- Fi2 digital color camera (Nikon Elements software). For postembryos, the prosoma was dissected with fine forceps, gradually immersed in 70% Glycerol/PBS-T and mounted on glass slides. Postembryos were imaged using an Olympus DP70 color camera mounted on an Olympus BX60 epifluorescence compound microscope.

Acknowledgements

Microscopy was performed at the Newcomb Imaging Center, Department of Botany, University of Wisconsin-Madison. Sequencing was performed at the UW-Madison Biotechnology Center. Access to computing nodes for intensive tasks was provided by the Center for High Throughput Computing (CHTC) and the Bioinformatics Resource Center (BRC) of the University of Wisconsin–Madison. Specimens were collected under permit 2018/42037, issued by the Israel National Parks Authority to E.G.R. Fieldwork in Israel was supported by a National Geographic Society Expeditions Council grant no. NGS-271R-18 to J.A.B. This work was supported by National Science Foundation (grant no. IOS-1552610) to P.P.S.

References

Akiyama-Oda, Y., & Oda, H. (2006). Axis specification in the spider embryo: *dpp* is required for radial-to-axial symmetry transformation and *sog* for ventral patterning. *Development*, *133*(12), 2347–2357. http://doi.org/10.1242/dev.02400

Arendt, D., Tessmar, K., Medeiros de Campos-Baptista, M. I., Dorresteijn, A., & Wittbrodt, J. (2002). Development of pigment-cup eyes in the polychaete *Platynereis dumerilii* and evolutionary conservation of larval eyes in bilateria. *Development*, *129*(5), 1143–1154.

Ballesteros, J. A., & Sharma, P. P. (2019). A Critical Appraisal of the Placement of Xiphosura (Chelicerata) with Account of Known Sources of Phylogenetic Error. *Systematic Biology*. http://doi.org/10.1093/sysbio/syz011

Ballesteros, J. A., Santibáñez López, C. E., Kováč, Ľ., Gavish-Regev, E., & Sharma, P. P. (2019). Ordered phylogenomic subsampling enables diagnosis of systematic errors in the placement of the enigmatic arachnid order Palpigradi. *Proceedings. Biological Sciences*, *286*(1917), 20192426. http://doi.org/10.1098/rspb.2019.2426

Barnett, A. A., & Thomas, R. H. (2012). The delineation of the fourth walking leg segment is temporally linked to posterior segmentation in the mite *Archegozetes longisetosus* (Acari: Oribatida, Trhypochthoniidae). *Evolution & Development*, *14*(4), 383–392.

http://doi.org/10.1111/j.1525-142X.2012.00556.x
Barnett, A. A., & Thomas, R. H. (2013a). Posterior Hox gene reduction in an arthropod: *Ultrabithorax* and *Abdominal-B* are expressed in a single segment in the mite *Archegozetes longisetosus*. *EvoDevo*, *4*(1), 23. http://doi.org/10.1186/2041-9139-4-23
Barnett, A. A., & Thomas, R. H. (2013b). The expression of limb gap genes in the mite *Archegozetes longisetosus* reveals differential patterning mechanisms in chelicerates. *Evolution & Development*, *15*(4), 280–292. http://doi.org/10.1111/ede.12038
Bebenek, I. G., Gates, R. D., Morris, J., Hartenstein, V., & Jacobs, D. K. (2004). *sine oculis* in basal Metazoa. *Development Genes and Evolution*, *214*(7), 342–351. http://doi.org/10.1007/s00427-004-0407-3
Bolger, A. M., Lohse, M., & Usadel, B. (2014). Trimmomatic: a flexible trimmer for Illumina sequence data. *Bioinformatics*, *30*(15), 2114–2120. http://doi.org/10.1093/bioinformatics/btu170
Bradic, M., Teotónio, H., & Borowsky, R. L. (2013). The Population Genomics of Repeated Evolution in the Blind Cavefish *Astyanax mexicanus*. *Molecular Biology and Evolution*, *30*(11), 2383–2400. http://doi.org/10.1093/molbev/mst136
Byrne, M., Koop, D., Morris, V. B., Chui, J., Wray, G. A., & Cisternas, P. (2017). Expression of genes and proteins of the Pax-Six-Eya-Dach network in the metamorphic sea urchin: Insights into development of the enigmatic echinoderm body plan and sensory structures. *Developmental Dynamics*, *247*(1), 239–249. http://doi.org/10.1002/dvdy.24584
Cagan, R. (2009). Chapter 5 - Principles of *Drosophila* Eye Differentiation. In *Current Topics in Developmental Biology* (Vol. 89, pp. 115–135). Elsevier. http://doi.org/10.1016/S0070-2153(09)89005-4
Capella-Gutiérrez, S., Silla-Martínez, J. M., & Gabaldón, T. (2009). trimAl: a tool for automated alignment trimming in large-scale phylogenetic analyses. *Bioinformatics*, *25*(15), 1972–1973. http://doi.org/10.1093/bioinformatics/btp348
Carroll, S. B. (2008). Evo-Devo and an Expanding Evolutionary Synthesis: A Genetic Theory of Morphological Evolution. *Cell*, *134*(1), 25–36. http://doi.org/10.1016/j.cell.2008.06.030
Coghill, L. M., Darrin Hulsey, C., Chaves-Campos, J., García de Leon, F. J., & Johnson, S. G. (2014). Next generation phylogeography of cave and surface *Astyanax mexicanus*. *Molecular Phylogenetics and Evolution*, *79*, 368–374. http://doi.org/10.1016/j.ympev.2014.06.029
Cruz-López, J. A., Proud, D. N., & Pérez-González, A. (2016). When troglomorphism dupes taxonomists: morphology and molecules reveal the first pyramidopid harvestman (Arachnida, Opiliones, Pyramidopidae) from the New World. *Zoological Journal of the Linnean Society*, *177*(3), 602–620. http://doi.org/10.1111/zoj.12382
Daly, I. M., How, M. J., Partridge, J. C., & Roberts, N. W. (2018). Complex gaze stabilization in mantis shrimp. *Proceedings of the Royal Society B: Biological Sciences*, *285*(1878). http://doi.org/10.1098/rspb.2018.0594
Derkarabetian, S., Steinmann, D. B., & Hedin, M. (2010). Repeated and time-correlated morphological convergence in cave-dwelling harvestmen (Opiliones, Laniatores) from montane Western North America. *PLoS ONE*, *5*(5), e10388. http://doi.org/10.1371/journal.pone.0010388
Esposito, L. A., Bloom, T., Caicedo-Quiroga, L., Alicea-Serrano, A. M., Sánchez-Ruíz, J. A., May-Collado, L. J., et al. (2015). Islands within islands: Diversification of tailless whip spiders (Amblypygi, *Phrynus*) in Caribbean caves. *Molecular Phylogenetics and Evolution*, *93*(C), 107–117. http://doi.org/10.1016/j.ympev.2015.07.005
Finn, R. D., Clements, J., Arndt, W., Miller, B. L., Wheeler, T. J., Schreiber, F., et al. (2015). HMMER web server: 2015 update. *Nucleic Acids Research*, *43*(W1), W30–8.

http://doi.org/10.1093/nar/gkv397
Foelix, R. (2011). Biology of Spiders (Third Edition). Oxford: Oxford University Press.
Garwood, R. J., Sharma, P. P., Dunlop, J. A., & Giribet, G. (2014). A Paleozoic Stem Group to Mite Harvestmen Revealed through Integration of Phylogenetics and Development. *Current Biology*, *24*(9), 1–7. http://doi.org/10.1016/j.cub.2014.03.039
Gehring, W. J., & Ikeo, K. (1999). *Pax 6*: mastering eye morphogenesis and eye evolution. *Trends in Genetics : TIG*, *15*(9), 371–377. http://doi.org/10.1016/s0168-9525(99)01776-x
Giribet, G. (2018). Current views on chelicerate phylogeny—A tribute to Peter Weygoldt. *Zoologischer Anzeiger - a Journal of Comparative Zoology*, *273*, 7–13. http://doi.org/10.1016/j.jcz.2018.01.004
Grabherr, M. G., Haas, B. J., Yassour, M., Levin, J. Z., Thompson, D. A., Amit, I., et al. (2011). Full-length transcriptome assembly from RNA-Seq data without a reference genome. *Nature Biotechnology*, *29*(7), 644–652. http://doi.org/10.1038/nbt.1883
Grbić, M., Khila, A., Lee, K.-Z., Bjelica, A., Grbić, V., Whistlecraft, J., et al. (2007). Mity model: *Tetranychus urticae*, a candidate for chelicerate model organism. *BioEssays*, *29*(5), 489–496. http://doi.org/10.1002/bies.20564
Grbić, M., Van Leeuwen, T., Clark, R. M., Rombauts, S., Rouzé, P., Grbić, V., et al. (2011). The genome of *Tetranychus urticae* reveals herbivorous pest adaptations. *Nature*, *479*(7374), 487–492. http://doi.org/10.1038/nature10640
Gulia-Nuss, M., Nuss, A. B., Meyer, J. M., Sonenshine, D. E., Roe, R. M., Waterhouse, R. M., et al. (2016). Genomic insights into the *Ixodes scapularis* tick vector of Lyme disease. *Nature Communications*, *7*(1), 10507–13. http://doi.org/10.1038/ncomms10507
Harland, D. P., Li, D., & Jackson, R. R. (2012). How jumping spiders see the world. http://doi.org/10.1093/acprof:oso/9780195334654.003.0010
Harvey, M. S. (2002). The neglected cousins: What do we know about the smaller arachnid orders? *Journal of Arachnology*, *30*(2), 357–372. http://doi.org/10.1636/0161-8202(2002)030[0357:TNCWDW]2.0.CO;2
Harvey, M. S. (2007). The smaller arachnid orders: Diversity, descriptions and distributions from Linnaeus to the present (1758 to 2007). *Zootaxa*, *1668*(1668), 363–380. http://doi.org/10.11646/zootaxa.1668.1.19
Hedin, M., & Thomas, S. M. (2010). Molecular systematics of eastern North American Phalangodidae (Arachnida: Opiliones: Laniatores), demonstrating convergent morphological evolution in caves. *Molecular Phylogenetics and Evolution*, *54*(1), 107–121. http://doi.org/10.1016/j.ympev.2009.08.020
Herman, A., Brandvain, Y., Weagley, J., Jeffery, W. R., Keene, A. C., Kono, T. J. Y., et al. (2018). The role of gene flow in rapid and repeated evolution of cave-related traits in Mexican tetra, *Astyanax mexicanus*. *Molecular Ecology*, *27*(22), 4397–4416. http://doi.org/10.1111/mec.14877
Homann, H. (1971). Die Augen der Araneae. *Zeitschrift Für Morphologie Der Tiere*, *69*(3), 201–272. http://doi.org/10.1007/BF00277623
Howarth, F. G. (1993). High-stress subterranean habitats and evolutionary change in cave-inhabiting arthropods. *The American Naturalist*, *142 Suppl 1*(Suppl.), S65–77. http://doi.org/10.1086/285523
Hoy, M. A., Waterhouse, R. M., Wu, K., Estep, A. S., Ioannidis, P., Palmer, W. J., et al. (2016). Genome Sequencing of the Phytoseiid Predatory Mite *Metaseiulus occidentalis* Reveals Completely Atomized Hox Genes and Superdynamic Intron Evolution. *Genome Biology and Evolution*, *8*(6), 1762–1775. http://doi.org/10.1093/gbe/evw048
Jeffery, W. R. (2009). Chapter 8. Evolution and development in the cavefish *Astyanax*. *Current Topics in Developmental Biology*, *86*, 191–221. http://doi.org/10.1016/S0070-

2153(09)01008-4
Jemec, A., Škufca, D., Prevorčnik, S., Fišer, Ž., & Zidar, P. (2017). Comparative study of acetylcholinesterase and glutathione S-transferase activities of closely related cave and surface *Asellus aquaticus* (Isopoda: Crustacea). *PLoS ONE*, *12*(5), e0176746–14. http://doi.org/10.1371/journal.pone.0176746
Juan, C., Guzik, M. T., Jaume, D., & Cooper, S. J. B. (2010). Evolution in caves: Darwin's 'wrecks of ancient life' in the molecular era. *Molecular Ecology*, *19*(18), 3865–3880. http://doi.org/10.1111/j.1365-294X.2010.04759.x
Katoh, K., & Standley, D. M. (2013). MAFFT multiple sequence alignment software version 7: improvements in performance and usability. *Molecular Biology and Evolution*, *30*(4), 772–780. http://doi.org/10.1093/molbev/mst010
Kenny, N. J., Chan, K. W., Nong, W., Qu, Z., Maeso, I., Yip, H. Y., et al. (2015). Ancestral whole-genome duplication in the marine chelicerate horseshoe crabs. *Heredity*, *116*(2), 190–199. http://doi.org/10.1038/hdy.2015.89
Khadjeh, S., Turetzek, N., Pechmann, M., Schwager, E. E., Wimmer, E. A., Damen, W. G. M., & Prpic, N. M. (2012). Divergent role of the Hox gene *Antennapedia* in spiders is responsible for the convergent evolution of abdominal limb repression. *Proceedings of the National Academy of Sciences*, *109*(13), 4921–4926. http://doi.org/10.1073/pnas.1116421109
Koressaar, T., & Remm, M. (2007). Enhancements and modifications of primer design program Primer3. *Bioinformatics*, *23*(10), 1289–1291. http://doi.org/10.1093/bioinformatics/btm091
Kumar, J. P. (2009). The molecular circuitry governing retinal determination. *Biochimica Et Biophysica Acta (BBA) - Gene Regulatory Mechanisms*, *1789*(4), 306–314. http://doi.org/10.1016/j.bbagrm.2008.10.001
Land, M. F. (1985). The Morphology and Optics of Spider Eyes. In *Neurobiology of Arachnids* (Vol. 189, pp. 53–78). Berlin, Heidelberg: Springer, Berlin, Heidelberg. http://doi.org/10.1007/978-3-642-70348-5_4
Leite, D. J., Baudouin-Gonzalez, L., Iwasaki-Yokozawa, S., Lozano-Fernandez, J., Turetzek, N., Akiyama-Oda, Y., et al. (2018). Homeobox Gene Duplication and Divergence in Arachnids. *Molecular Biology and Evolution*, *35*(9), 2240–2253. http://doi.org/10.1093/molbev/msy125
Love, M. I., Huber, W., & Anders, S. (2014). Moderated estimation of fold change and dispersion for RNA-seq data with DESeq2. *Genome Biology*, *15*(12), 31–21. http://doi.org/10.1186/s13059-014-0550-8
Lozano-Fernandez, J., Tanner, A. R., Giacomelli, M., Carton, R., Vinther, J., Edgecombe, G. D., & Pisani, D. (2019). Increasing species sampling in chelicerate genomic-scale datasets provides support for monophyly of Acari and Arachnida. *Nature Communications*, 1–8. http://doi.org/10.1038/s41467-019-10244-7
Mammola, S., & Isaia, M. (2017). Spiders in caves. *Proceedings of the Royal Society B: Biological Sciences*, *284*(1853), 20170193–10. http://doi.org/10.1098/rspb.2017.0193
Mammola, S., Arnedo, M. A., Pantini, P., Piano, E., Chiappetta, N., & Isaia, M. (2018a). Ecological speciation in darkness? Spatial niche partitioning in sibling subterranean spiders (Araneae: Linyphiidae: Troglohyphantes). *Invertebrate Systematics*, *32*(5), 1069–1082. http://doi.org/10.1071/IS17090
Mammola, S., Cardoso, P., Ribera, C., Pavlek, M., & Isaia, M. (2018b). A synthesis on cave-dwelling spiders in Europe. *Journal of Zoological Systematics and Evolutionary Research*, *56*(3), 301–316. http://doi.org/10.1111/jzs.12201
Mammola, S., Mazzuca, P., Pantini, P., Isaia, M., & Arnedo, M. A. (2017). Advances in the systematics of the spider genus *Troglohyphantes* (Araneae, Linyphiidae). *Systematics*

and Biodiversity, *15*(4), 307–326. http://doi.org/10.1080/14772000.2016.1254304

Marshall, J., Cronin, T. W., & Kleinlogel, S. (2007). Stomatopod eye structure and function: A review. *Arthropod Structure & Development*, *36*(4), 420–448. http://doi.org/10.1016/j.asd.2007.01.006

Miranda, G. S., Aharon, S., Gavish-Regev, E., Giupponi, A. P. L., & Wizen, G. (2016). A new species of *Charinus* Simon, 1892 (Arachnida: Amblypygi: Charinidae) from Israel and new records of *C. ioanniticus* (Kritscher, 1959). *European Journal of Taxonomy*, (234), 1–18. http://doi.org/10.5852/ejt.2016.234

Mittmann, B., & Wolff, C. (2012). Embryonic development and staging of the cobweb spider *Parasteatoda tepidariorum* C. L. Koch, 1841 (syn.: *Achaearanea tepidariorum*; Araneomorphae; Theridiidae). *Development Genes and Evolution*, *222*(4), 189–216. http://doi.org/10.1007/s00427-012-0401-0

Mojaddidi, H., Fernandez, F. E., Erickson, P. A., & Protas, M. E. (2018). Embryonic origin and genetic basis of cave associated phenotypes in the isopod crustacean *Asellus aquaticus*. *Scientific Reports*, 1–12. http://doi.org/10.1038/s41598-018-34405-8

Morehouse, N. I., Buschbeck, E. K., Zurek, D. B., Steck, M., & Porter, M. L. (2017). Molecular Evolution of Spider Vision: New Opportunities, Familiar Players. *Biol Bull*, *233*(1), 21–38. http://doi.org/10.1086/693977

Nguyen, L.-T., Schmidt, H. A., Haeseler, von, A., & Minh, B. Q. (2015). IQ-TREE: a fast and effective stochastic algorithm for estimating maximum-likelihood phylogenies. *Molecular Biology and Evolution*, *32*(1), 268–274. http://doi.org/10.1093/molbev/msu300

Nolan, E. D., Santibáñez López, C. E., & Sharma, P. P. (2020). Developmental gene expression as a phylogenetic data class: support for the monophyly of Arachnopulmonata. *Development Genes and Evolution*, *230*(2), 137–153. http://doi.org/10.1007/s00427-019-00644-6

Nossa, C. W., Havlak, P., Yue, J.-X., Lv, J., Vincent, K. Y., Brockmann, H. J., & Putnam, N. H. (2014). Joint assembly and genetic mapping of the Atlantic horseshoe crab genome reveals ancient whole genome duplication. *GigaScience*, *3*(1), 708–21. http://doi.org/10.1186/2047-217X-3-9

Oda, H., & Akiyama-Oda, Y. (2020). The common house spider *Parasteatoda tepidariorum*. *EvoDevo*, 1–7. http://doi.org/10.1186/s13227-020-00152-z

Paese, C. L. B., Leite, D. J., Schönauer, A., McGregor, A. P., & Russell, S. (2018). Duplication and expression of Sox genes in spiders, 1–14. http://doi.org/10.1186/s12862-018-1337-4

Patro, R., Duggal, G., Love, M. I., Irizarry, R. A., & Kingsford, C. (2017). Salmon provides fast and bias-aware quantification of transcript expression. *Nature Publishing Group*, *14*(4), 417–419. http://doi.org/10.1038/nmeth.4197

Paulus, H. F. (1979). Eye structure and the monophyly of the Arthropoda. In "Arthropod Phylogeny"(A. PGupta, Ed.) pp. 299–383.

Pechmann, M. (2016). Formation of the germ-disc in spider embryos by a condensation-like mechanism. *Frontiers in Zoology*, *13*(1), 35. http://doi.org/10.1186/s12983-016-0166-9

Pechmann, M., McGregor, A. P., Schwager, E. E., Feitosa, N. M., & Damen, W. G. M. (2009). Dynamic gene expression is required for anterior regionalization in a spider. *Proceedings of the National Academy of Sciences of the United States of America*, *106*(5), 1468–1472. http://doi.org/10.1073/pnas.0811150106

Pineda, D., Gonzalez, J., Callaerts, P., Ikeo, K., Gehring, W. J., & Salo, E. (2000). Searching for the prototypic eye genetic network: *Sine oculis* is essential for eye regeneration in planarians. *Proceedings of the National Academy of Sciences*, *97*(9), 4525–4529. http://doi.org/10.1073/pnas.97.9.4525

Porter, M. L., Dittmar, K., & Pérez-Losada, M. (2007). How long does evolution of the troglomorphic form take? Estimating divergence times in *Astyanax mexicanus*. *Acta Carsologica*, *36*(1), 173–182. http://doi.org/10.3986/ac.v36i1.219

Posnien, N., Zeng, V., Schwager, E. E., Pechmann, M., Hilbrant, M., Keefe, J. D., et al. (2014). A Comprehensive Reference Transcriptome Resource for the Common House Spider *Parasteatoda tepidariorum*. *PLoS ONE*, *9*(8), e104885–20. http://doi.org/10.1371/journal.pone.0104885

Protas, M. E., Hersey, C., Kochanek, D., Zhou, Y., Wilkens, H., Jeffery, W. R., et al. (2005). Genetic analysis of cavefish reveals molecular convergence in the evolution of albinism. *Nature Genetics*, *38*(1), 107–111. http://doi.org/10.1038/ng1700

Protas, M. E., Trontelj, P., & Patel, N. H. (2011). Genetic basis of eye and pigment loss in the cave crustacean, *Asellus aquaticus*. *Proceedings of the National Academy of Sciences of the United States of America*, *108*(14), 5702–5707. http://doi.org/10.1073/pnas.1013850108

Protas, M., & Jeffery, W. R. (2012). Evolution and development in cave animals: from fish to crustaceans. *Wiley Interdisciplinary Reviews: Developmental Biology*, *1*(6), 823–845. http://doi.org/10.1002/wdev.61

Re, C., Fišer, Ž., Perez, J., Tacdol, A., Trontelj, P., & Protas, M. E. (2018). Common Genetic Basis of Eye and Pigment Loss in Two Distinct Cave Populations of the Isopod Crustacean *Asellus aquaticus*. *Integrative and Comparative Biology*, *58*(3), 421–430. http://doi.org/10.1093/icb/icy028

Riddle, M. R., Aspiras, A. C., Gaudenz, K., Peuß, R., Sung, J. Y., Martineau, B., et al. (2018). Insulin resistance in cavefish as an adaptation to a nutrient-limited environment. *Nature*, 1–19. http://doi.org/10.1038/nature26136

Rivera, A., Winters, I., Rued, A., Ding, S., Posfai, D., Cieniewicz, B., et al. (2013). The evolution and function of the Pax/Six regulatory network in sponges. *Evolution & Development*, *15*(3), 186–196. http://doi.org/10.1111/ede.12032

Rota-Stabelli, O., Campbell, L., Brinkmann, H., Edgecombe, G. D., Longhorn, S. J., Peterson, K. J., et al. (2010). A congruent solution to arthropod phylogeny: phylogenomics, microRNAs and morphology support monophyletic Mandibulata. *Proceedings of the Royal Society B: Biological Sciences*, *278*(1703), 298–306. http://doi.org/10.1098/rspb.2010.0590

Samadi, L., Schmid, A., & Eriksson, B. J. (2015). Differential expression of retinal determination genes in the principal and secondary eyes of *Cupiennius salei* Keyserling (1877). *EvoDevo*, *6*(1), 16–17. http://doi.org/10.1186/s13227-015-0010-x

Sandve, S. R., Rohlfs, R. V., & Hvidsten, T. R. (2018). Subfunctionalization versus neofunctionalization after whole-genome duplication. *Nature Publishing Group*, *50*(7), 908–909. http://doi.org/10.1038/s41588-018-0162-4

Santibáñez López, C. E., Francke, O. F., & Prendini, L. (2014). Shining a light into the world's deepest caves: phylogenetic systematics of the troglobiotic scorpion genus *Alacran* Francke, 1982 (Typhlochactidae:Alacraninae). *Invertebrate Systematics*, *28*(6), 643–664. http://doi.org/10.1071/IS14035

Santos, V. T., Ribeiro, L., Fraga, A., de Barros, C. M., Campos, E., Moraes, J., et al. (2013). The embryogenesis of the Tick *Rhipicephalus* (*Boophilus*) *microplus*: The establishment of a new chelicerate model system. *Genesis*, *51*(12), 803–818. http://doi.org/10.1002/dvg.22717

Schacht, M. I., Schomburg, C., & Bucher, G. (2020). *six3* acts upstream of *foxQ2* in labrum and neural development in the spider *Parasteatoda tepidariorum*. *Development Genes and Evolution*, *230*(2), 95–104. http://doi.org/10.1007/s00427-020-00654-9

Schomburg, C., Turetzek, N., Schacht, M. I., Schneider, J., Kirfel, P., Prpic, N.-M., &

975 Posnien, N. (2015). Molecular characterization and embryonic origin of the eyes in the
976 common house spider *Parasteatoda tepidariorum*. *EvoDevo*, *6*(1), 15.
977 http://doi.org/10.1186/s13227-015-0011-9
978 Schwager, E. E., Pechmann, M., Feitosa, N. M., McGregor, A. P., & Damen, W. G. M.
979 (2009). *hunchback* functions as a segmentation gene in the spider *Achaearanea*
980 *tepidariorum*. *Current Biology : CB*, *19*(16), 1333–1340.
981 http://doi.org/10.1016/j.cub.2009.06.061
982 Schwager, E. E., Sharma, P. P., Clarke, T., Leite, D. J., Wierschin, T., Pechmann, M., et al.
983 (2017). The house spider genome reveals an ancient whole-genome duplication during
984 arachnid evolution. *BMC Biology*, *15*(1), 62. http://doi.org/10.1186/s12915-017-0399-x
985 Setton, E. V. W., March, L. E., Nolan, E. D., Jones, T. E., Cho, H., Wheeler, W. C., et al.
986 (2017). Expression and function of *spineless* orthologs correlate with distal deutocerebral
987 appendage morphology across Arthropoda. *Developmental Biology*, *430*(1), 224–236.
988 http://doi.org/10.1016/j.ydbio.2017.07.016
989 Sharma, P. P., Kaluziak, S. T., Pérez-Porro, A. R., González, V. L., Hormiga, G., Wheeler,
990 W. C., & Giribet, G. (2014a). Phylogenomic interrogation of Arachnida reveals systemic
991 conflicts in phylogenetic signal. *Molecular Biology and Evolution*, *31*(11), 2963–2984.
992 http://doi.org/10.1093/molbev/msu235
993 Sharma, P. P., Santiago, M. A., González-Santillán, E., Monod, L., & Wheeler, W. C.
994 (2015a). Evidence of duplicated Hox genes in the most recent common ancestor of extant
995 scorpions. *Evolution & Development*, *17*(6), 347–355. http://doi.org/10.1111/ede.12166
996 Sharma, P. P., Schwager, E. E., Extavour, C. G., & Giribet, G. (2012). Hox gene expression
997 in the harvestman *Phalangium opilio* reveals divergent patterning of the chelicerate
998 opisthosoma. *Evolution & Development*, *14*(5), 450–463. http://doi.org/10.1111/j.1525-
999 142X.2012.00565.x
1000 Sharma, P. P., Schwager, E. E., Extavour, C. G., & Wheeler, W. C. (2014b). Hox gene
1001 duplications correlate with posterior heteronomy in scorpions. *Proceedings. Biological*
1002 *Sciences*, *281*(1792), 20140661–20140661. http://doi.org/10.1098/rspb.2014.0661
1003 Sharma, P. P., Schwager, E. E., Giribet, G., Jockusch, E. L., & Extavour, C. G. (2013).
1004 *Distal-less* and *dachshund* pattern both plesiomorphic and apomorphic structures in
1005 chelicerates: RNA interference in the harvestman *Phalangium opilio* (Opiliones).
1006 *Evolution & Development*, *15*(4), 228–242. http://doi.org/10.1111/ede.12029
1007 Sharma, P. P., Tarazona, O. A., Lopez, D. H., Schwager, E. E., Cohn, M. J., Wheeler, W. C.,
1008 & Extavour, C. G. (2015b). A conserved genetic mechanism specifies deutocerebral
1009 appendage identity in insects and arachnids. *Proceedings of the Royal Society B:*
1010 *Biological Sciences*, *282*(1808), 20150698–20150698.
1011 http://doi.org/10.1098/rspb.2015.0698
1012 Shubin, N., Tabin, C., & Carroll, S. (2009). Deep homology and the origins of evolutionary
1013 novelty. *Nature*, *457*(7231), 818–823. http://doi.org/10.1038/nature07891
1014 Shull, L. C., Sen, R., Menzel, J., Goyama, S., Kurokawa, M., & Artinger, K. B. (2020). The
1015 conserved and divergent roles of Prdm3 and Prdm16 in zebrafish and mouse craniofacial
1016 development. *Developmental Biology*. http://doi.org/10.1016/j.ydbio.2020.02.006
1017 Smrž, J., Kováč, Ľ., Mikeš, J., & Lukešová, A. (2013). Microwhip Scorpions (Palpigradi)
1018 Feed on Heterotrophic Cyanobacteria in Slovak Caves - A Curiosity among Arachnida.
1019 *PLoS ONE*, *8*(10), e75989. http://doi.org/10.1371/journal.pone.0075989
1020 Soneson, C., Love, M. I., & Robinson, M. D. (2015). Differential analyses for RNA-seq:
1021 transcript-level estimates improve gene-level inferences. *F1000Research*, *4*, 1521.
1022 http://doi.org/10.12688/f1000research.7563.1
1023 Stahl, B. A., Gross, J. B., Speiser, D. I., Oakley, T. H., Patel, N. H., Gould, D. B., & Protas,
1024 M. E. (2015). A Transcriptomic Analysis of Cave, Surface, and Hybrid Isopod

Crustaceans of the Species *Asellus aquaticus*. *PLoS ONE*, *10*(10), e0140484–14. http://doi.org/10.1371/journal.pone.0140484

Strickler, A. G., Yamamoto, Y., & Jeffery, W. R. (2001). Early and late changes in *Pax6* expression accompany eye degeneration during cavefish development. *Development Genes and Evolution*, *211*(3), 138–144. http://doi.org/10.1007/s004270000123

Takagi, A., Kurita, K., Terasawa, T., Nakamura, T., Bando, T., Moriyama, Y., et al. (2012). Functional analysis of the role of *eyes absent* and *sine oculis* in the developing eye of the cricket *Gryllus bimaculatus*. *Development, Growth & Differentiation*, *54*(2), 227–240. http://doi.org/10.1111/j.1440-169X.2011.01325.x

Telford, M. J., & Thomas, R. H. (1998). Expression of homeobox genes shows chelicerate arthropods retain their deutocerebral segment. *Proceedings of the National Academy of Sciences*, *95*(18), 10671–10675. http://doi.org/10.1073/pnas.95.18.10671

Thoen, H. H., How, M. J., Chiou, T.-H., & Marshall, J. (2014). A different form of color vision in mantis shrimp. *Science*, *343*(6169), 411–413. http://doi.org/10.1126/science.1245824

Turetzek, N., Pechmann, M., Schomburg, C., Schneider, J., & Prpic, N.-M. (2015). Neofunctionalization of a Duplicate *dachshund* Gene Underlies the Evolution of a Novel Leg Segment in Arachnids. *Molecular Biology and Evolution*, *33*(1), 109–121. http://doi.org/10.1093/molbev/msv200

Vopalensky, P., & Kozmik, Z. (2009). Eye evolution: common use and independent recruitment of genetic components. *Philosophical Transactions of the Royal Society B: Biological Sciences*, *364*(1531), 2819–2832. http://doi.org/10.1098/rstb.2009.0079

Waterhouse, R. M., Seppey, M., Simão, F. A., Manni, M., Ioannidis, P., Klioutchnikov, G., et al. (2017). BUSCO Applications from Quality Assessments to Gene Prediction and Phylogenomics. *Molecular Biology and Evolution*, *35*(3), 543–548. http://doi.org/10.1093/molbev/msx319

Weygoldt, P. (1975). Untersuchungen zur Embryologie und Morphologie der Geißelspinne *Tarantula marginemaculata* C. L. Koch (Arachnida, Amblypygi, Tarantulidae). *Zoomorphologie*, *82*, 137–199.

Weygoldt, P. (2000). Whip Spiders (Chelicerata: Amblypygi). Their Biology, Morphology and Systematics. Apollo Books.

ZarinKamar, N., Yang, X., Bao, R., Friedrich, F., Beutel, R., & Friedrich, M. (2011). The *Pax* gene *eyegone* facilitates repression of eye development in *Tribolium*. *EvoDevo*, *2*(1), 8–15. http://doi.org/10.1186/2041-9139-2-8

Zhou, Y., Liang, Y., Yan, Q., Zhang, L., Chen, D., Ruan, L., et al. (2020). The draft genome of horseshoe crab *Tachypleus tridentatus* reveals its evolutionary scenario and well-developed innate immunity. *BMC Genomics*, *21*(1), 137–15. http://doi.org/10.1186/s12864-020-6488-1

Zurek, D. B., Cronin, T. W., Taylor, L. A., Byrne, K., Sullivan, M. L. G., & Morehouse, N. I. (2015). Spectral filtering enables trichromatic vision in colorful jumping spiders. *Current Biology*, *25*(10), R403–R404. http://doi.org/10.1016/j.cub.2015.03.033

1068 Figure 1: Species used in this study and their eye arrangement. A: Schematic representation
1069 of the eyes of *Charinus* whip spiders (Amblypygi) (upper), and the spider *Parasteatoda*
1070 *tepidariorum* (Araneae; lower). B: Live specimen of *C. ioanniticus* from Khirbet Haruba
1071 cave (Haruva cave). Inset: detail of the median eyes. C: Live specimen of *C. israelensis*
1072 from Mimlach cave. Inset: detail of the reduced median eyes. D: Live specimen of
1073 *Parasteatoda tepidariorum*, and schematic representation of the expression patterns of
1074 paralog pairs of *Ptep-sine oculis* (*soA*/*soB*), *Ptep-orthodenticle* (*otdA*/*otdB*), and *Ptep-*
1075 *Optix* (*OptixA*/*OptixB*) in the eyes. ME: median eyes; ALE: anterior lateral eyes; PLE:
1076 posterior lateral eyes; MLE: median lateral eyes; LE: lateral eyes.

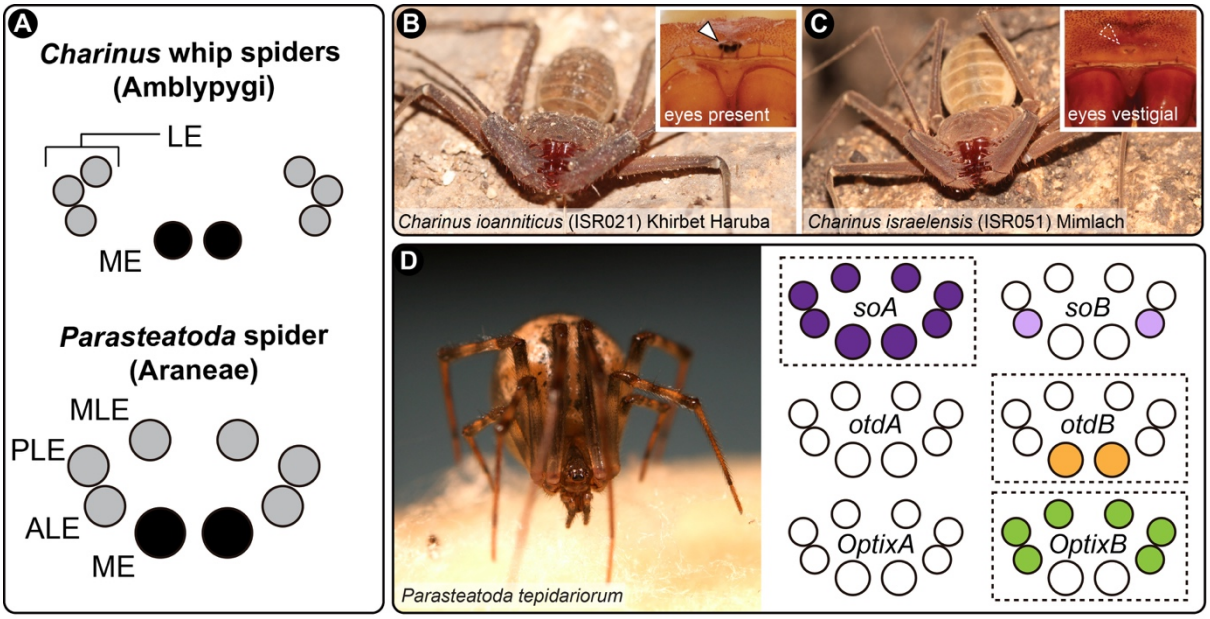

1077

1078 Figure 2: Phylogenetic distribution of Retinal Determination Gene Network (RDGN) genes
1079 in an insect (*Drosophila melanogaster*), a non-arachnopulmonate arachnid group
1080 (Acariformes: *Dinothrombium tinctorium*; *Tetranychus urticae*) and Arachnopulmonata
1081 (spider: *Parasteatoda tepidariorum*; scorpion: *Centruroides sculpturatus*), including
1082 newly discovered orthologs in *Charinus* whip spiders (Amblypygi). Colored squares
1083 indicate number of gene copies for each RDGN gene. Dotted squares indicate missing
1084 data, not gene loss. For comprehensive list of duplicated genes in Arachnopulmonata see
1085 Schwager et al. (2017) and Leite et al. 2018. Gene trees and alignments for each gene are
1086 available in SI Appendix Dataset S1.

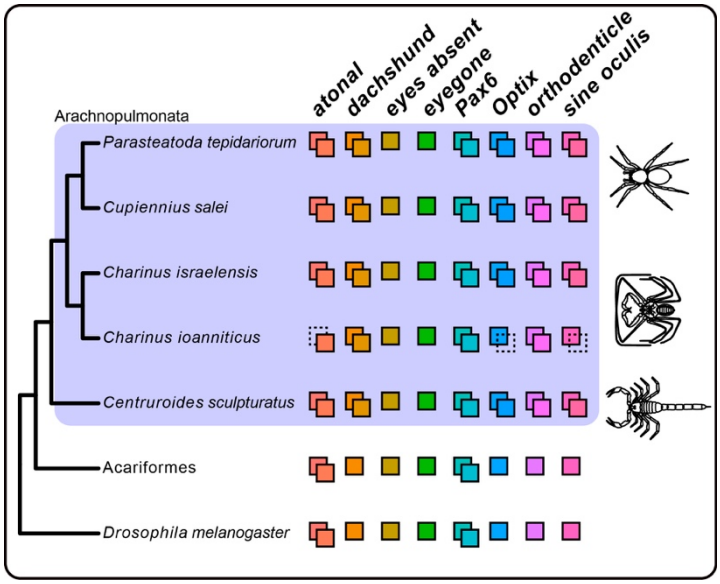

1087

1088

Figure 3: Differential gene expression analysis of Retinal Determination Gene Network (RDGN) genes in *Charinus* whip spider deutembryos. Bar graphs display $\log_2$ fold change of selected RDGN genes. Direction of differential gene expression always follows sample to the left. A: Comparison 1; Comparison between reads of early (pre-eyespot) and late deutembryos (eyespot) of the eye-bearing species *C. ioanniticus* mapped onto *C. ioanniticus* transcriptome. B: Comparison 2.1; Comparison between reads of early deutembryo of *C. ioanniticus* and early deutembryo of *C. israelensis* mapped onto *C. israelensis* transcriptome. B: Comparison 2.2; Comparison between reads of early deutembryo of *C. ioanniticus* and early deutembryo of *C. israelensis* mapped onto *C. ioanniticus* transcriptome. *atoA*/*B*: *atonalA*/*atonalB*; *dacA*/*B*: *dachshundA*/*B*; *eya*: *eyes absent*; *eyg*: *eyegone*; *otdA*/*B*: *orthodenticleA*/*B*; *soA*/*B*: *sine oculisA*/*B*. Asterisks denote genes that were differentially expressed with a $p_{adj}>0.05$. $\text{Log}_2\text{FC} = 0$ for *atoA*, *OptixB*, and *soB* for Comparison 1 and Comparison 2.2 are due to the absence of those paralogs in *C. ioanniticus* reference transcriptome.

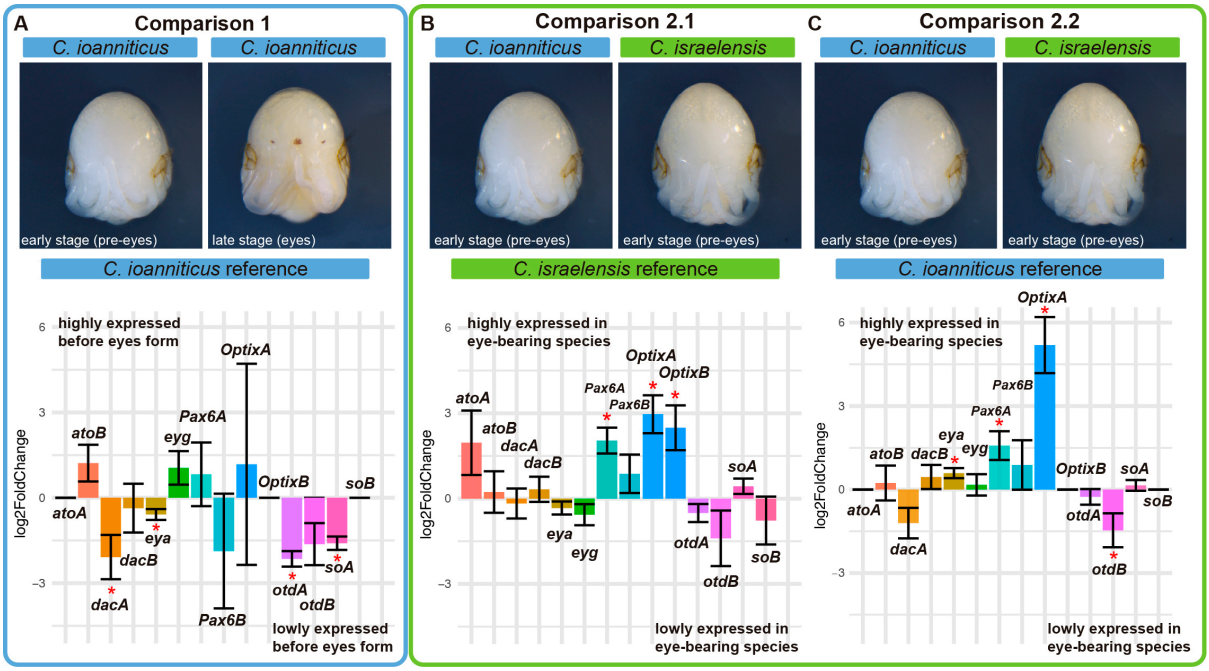

1105 Figure 4: In situ hybridization using DIG-labeled riboprobes for *Ptep-soA* in late embryos of
1106 the spider *Parasteatoda tepidariorum*. All embryos in frontal view. A–D: bright field
1107 images. A'–D': Same embryos, in Hoechst staining. A: Sense probe of a stage 14.2
1108 embryo (no signal). B: Antisense probe on a wild type stage 14.1 embryo. C: Antisense
1109 probe on a wild type stage 14.2 embryo. D: Antisense probe on a stage 14.2 embryo from
1110 the *Ptep-soA* dsRNA-injected treatment. *soA*: *sine oculis A*. White arrowhead: median
1111 eye; Black arrow: anterior lateral eye; White arrow: median lateral eye; Double white
1112 arrow: Posterior lateral eye. Dotted arrowhead/arrow indicate asymmetrical expression
1113 and eye defect. Sample sizes are indicated above each treatment.

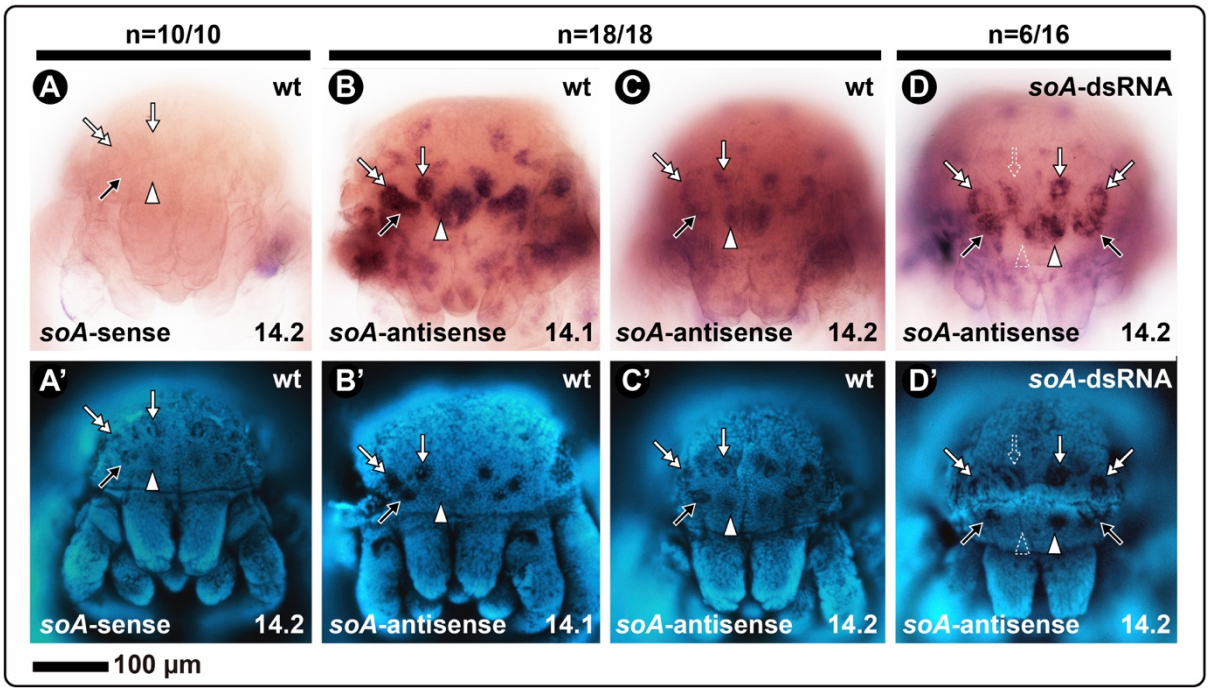

1114

1115
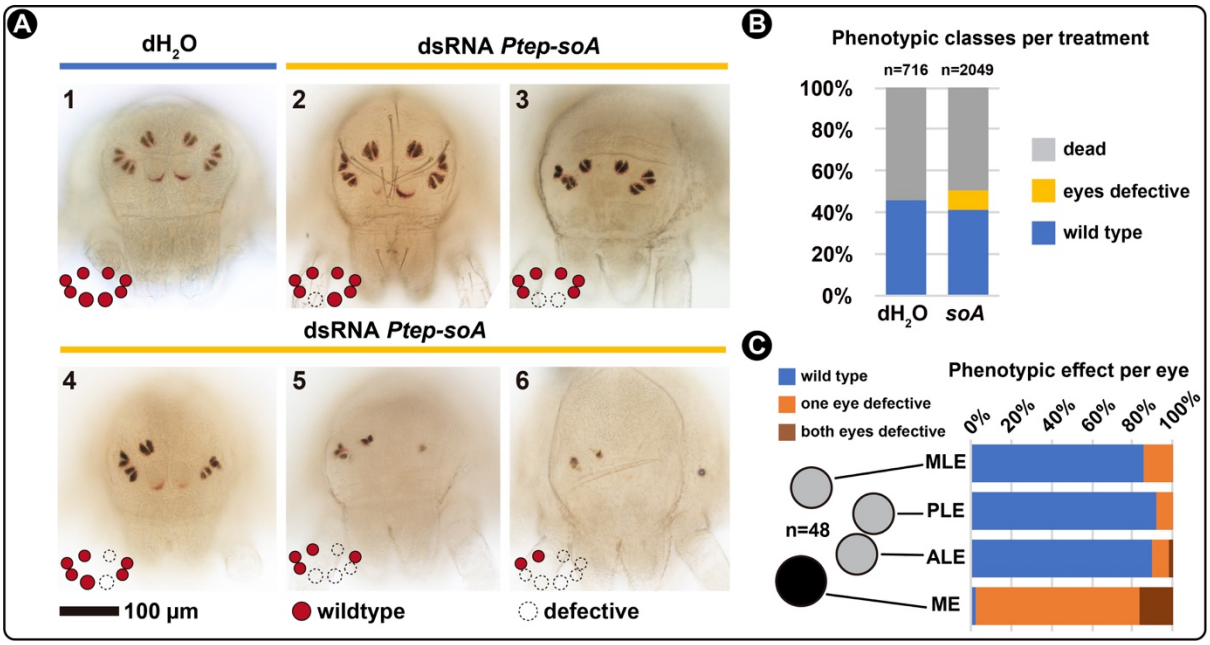
Figure 5: RNA interference against *Ptep-sine oculis A*. A: Bright field images of the spider *Parasteatoda tepidariorum* postembryos resulting from control treatment (dH_2O-injected, panel 1) and double stranded RNA (dsRNA) injected treatment (panels 2–6), in frontal view. B: Frequencies of each phenotypic class per treatment from the combined clutches of all females. See SI Appendix Fig. S13 for counts per clutch. C: Frequencies of symmetrical, asymmetrical, and wild type eyes quantified from a subset of 48 individuals with eye reduction phenotype. See SI Appendix Fig. S12 for figures of all specimens and coding, and Material and Methods for the scoring criteria. ME: median eyes; ALE: anterior lateral eyes; PLE: posterior lateral eyes; MLE: median lateral eyes. Schematics for the different eye types follows the nomenclature in Figure 1.